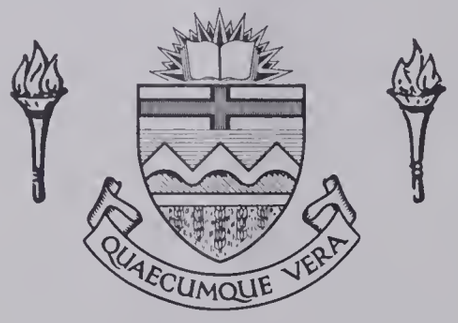

The University of Alberta
Printing Department
Edmonton, Alberta

UNIVERSITY OF ALBERTA
LIBRARY

Regulations Regarding Theses and Dissertations

Typescript copies of theses and dissertations for Master's and Doctor's degrees deposited in the University of Alberta Library, as the official Copy of the Faculty of Graduate Studies, may be consulted in the Reference Reading Room only.

A second copy is on deposit in the Department under whose supervision the work was done. Some Departments are willing to loan their copy to libraries, through the inter-library loan service of the University of Alberta Library.

These theses and dissertations are to be used only with due regard to the rights of the author. Written permission of the author and of the Department must be obtained through the University of Alberta Library when extended passages are copied. When permission has been granted, acknowledgement must appear in the published work.

This thesis or dissertation has been used in accordance with the above regulations by the persons listed below. The borrowing library is obligated to secure the signature of each user.

Please sign below:

Date	Signature	Institution

THE UNIVERSITY OF ALBERTA

STUDY OF STATES OF ^{33}Cl BELOW 3 MeV EXCITATION BY THE $^{32}S(d,n)^{33}Cl$ REACTION

by

© SAYED ALY EL-BAKR

A THESIS

SUBMITTED TO THE FACULTY OF GRADUATE STUDIES

IN PARTIAL FULFILLMENT OF THE REQUIREMENTS FOR THE DEGREE

OF MASTER OF SCIENCE

DEPARTMENT OF PHYSICS

EDMONTON, ALBERTA

FALL, 1969

UNIVERSITY OF ALBERTA

FACULTY OF GRADUATE STUDIES

The undersigned certify that they have read, and recommend to the Faculty of Graduate Studies for acceptance, a thesis entitled STUDY OF STATES OF ^{33}Cl BELOW 3 MeV EXCITATION BY THE $^{32}S(d,n)^{33}Cl$ REACTION submitted by Sayed Aly El-Bakr in partial fulfillment of the requirements for the degree of Master of Science.

ABSTRACT

The reaction $^{32}S(d,n)^{33}Cl$ has been investigated by the neutron time-of-flight method. Precise reaction Q-values and the corresponding excitation energies for the low-lying levels of ^{33}Cl have been measured. Angular distributions of the neutrons leading to the ground, 0.812, 2.688 and 2.851 MeV levels have been studied at E_d = 4.70 and 5.50 MeV. Angular distributions of the neutrons leading to the 1.993 and 2.351 MeV states have been measured at E_d = 4.54 and 4.70 MeV. The DWBA theory has been employed to determine the orbital angular momentum l of the captured proton. The Hauser-Feshbach calculations have been performed to see how important is the contribution from the compound nucleus formation. Reasonable agreement has been obtained between DWBA theory and experimental results. l-values of 2, 0, 3 and 1 have been obtained for the ground, 0.812, 2.688 and 2.851 MeV states, respectively. The absolute spectroscopic factors have been extracted and compared to shell model predictions. Qualitative agreement has been obtained.

ACKNOWLEDGEMENTS

I would like to express my thanks to Dr. W.J. McDonald under whose supervision this work was carried out; his pertinent remarks and directions were always useful. The deep involvement, encouragement and enthusiasm of Dr. G.C. Neilson in this work are gratefully acknowledged.

I wish to convey my special appreciation and gratitude to Dr. C. Glavina who spared no pains to share fully in every step of this project, and to whom I am most indebted for the experience I have gained during the course of this work. His mightly help, encouragement and pleasant personality are never forgotten.

The co-operating effort, in data taking, of Dr. J. Honsaker, Dr. K.V.K. Iyengar and Mr. T. Sharma is greatly appreciated.

Thanks are due to Dr. G. Roy, Mr. R. Humphries and Mr. W. Saunders for their great help in trying the elastic scattering experiment. I wish also to thank Mr. N. Davison who made available the Hauser-Feshbach computer code and his data on ^{17}F states.

The cooperative and friendly attitude of all the colleagues in the Nuclear Research Center are highly appreciated.

I would also put on record my gratefulness to Dr. W.K. Dawson and Mr. J.F. Easton, for providing an excellent data acquisition system. Thanks are also extended to Messrs. J.B. Elliott, L. Holm, P. Ford and the other members of the technical staff at the Nuclear Research Center.

I am indebted to Mrs. Marjorie Lybacki and Miss Audrey Forman for their careful typing of this thesis. My great appreciation is also due to Miss Elsie Hawirko for her heroic effort in making the last minute changes.

I would like to thank my wife, Mona, who has given me the support and sympathy any research worker needs.

Finally, I wish to acknowledge the financial support provided by the University of Alberta throughout the course of this work.

TABLE OF CONTENTS

TABLES

LIST OF FIGURES

CHAPTER I

INTRODUCTION

Nuclear reactions constitute one of the most powerful tools of nuclear spectroscopy, i.e., the mapping of nuclear energy levels. The level schemes, with all the pertinent information about each state, of course, constitute the most valuable data for testing theories of nuclear structure.

The present work reports on the low-lying states of ^{33}Cl as observed in the $^{32}S(d,n)^{33}Cl$ reaction. This reaction has been studied with low resolution by Middleton et al. (Mi 53), Macefield and Towle (Ma 60) and Mubarakmand and Macefield (Mu 67). In a (d,n) experiment done by Grandy et al. (Gr 68) in this laboratory on a ^{42}Ca target, which was contaminated with ^{32}S, a number of transitions to states in ^{33}Cl have been identified. The levels reported in (d,n), (^{3}He,d) and (p,γ) experiments on ^{32}S are presented in fig. 1-1. It is noticed that the levels at 2.11 and 2.53 MeV have been seen only in the (d,n) experiments, while the levels at 1.99 and 2.35 MeV have been observed only in the (^{3}He,d) and (p,γ) work. The level at 2.69 MeV, reported in (^{3}He,d) experiments, also has been seen in Grandy (d,n) work together with three new levels at 2.63, 3.24 and 3.27 MeV. The results of Grandy et al. are somewhat uncertain since ^{32}S was just a contaminant.

Figure 1-1. Levels of the mirror nuclei ^{33}Cl and ^{33}S as observed in different reactions.

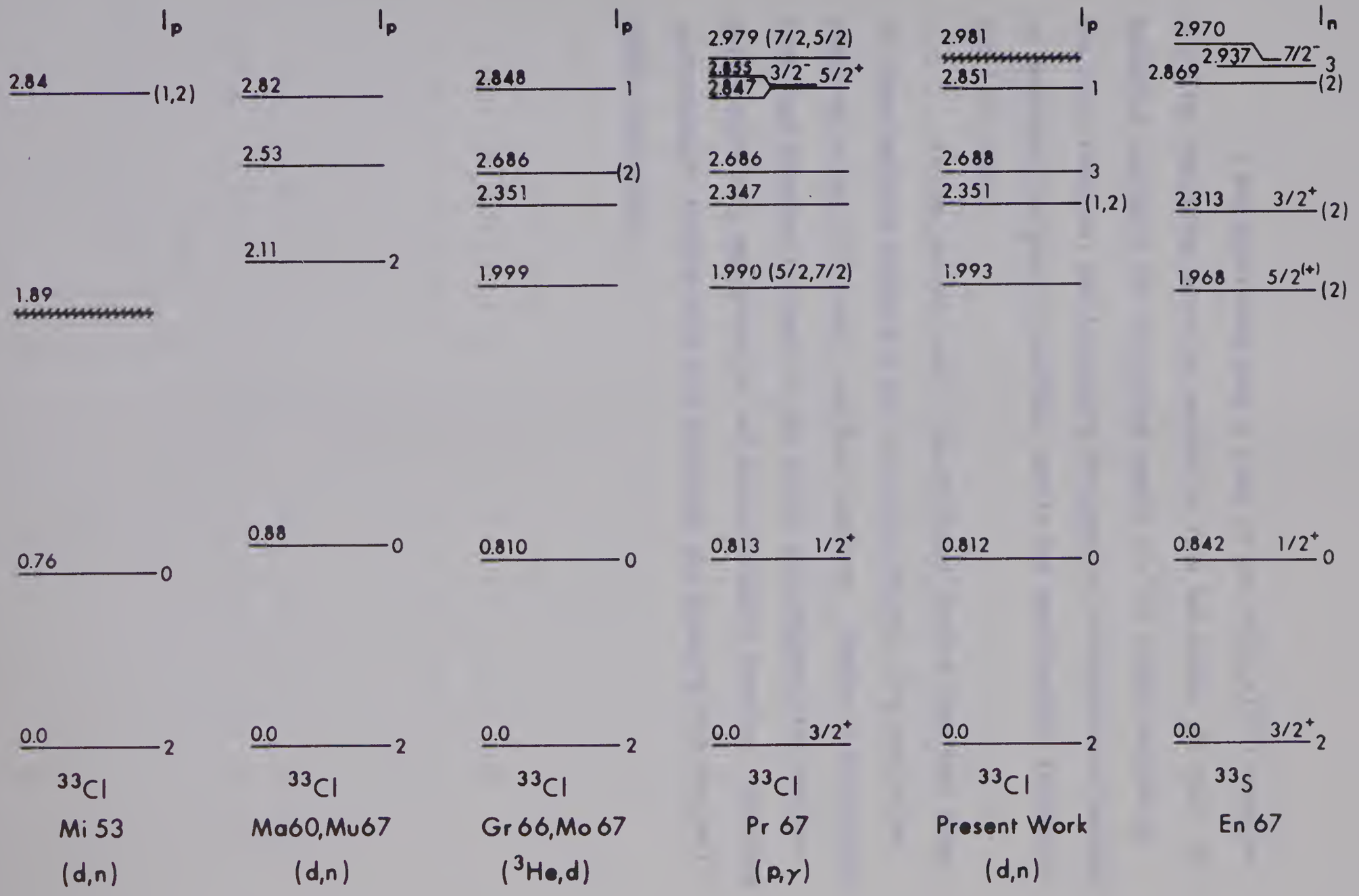
l_p
2.84
(1,2)
1.89
0.76
0
0.0
2
^{33}Cl
Mi 53
(d,n)
l_p
2.82
2.53
2.11
2
0.88
0
0.0
2
^{33}Cl
Ma60,Mu67
(d,n)
l_p
2.848
1
2.686
(2)
2.351
1.999
0.810
0
0.0
2
^{33}Cl
Gr 66,Mo 67
(^{3}He,d)
2.979 (7/2,5/2)
2.855 3/2$^-$ 5/2$^+$
2.847
2.686
2.347
1.990 (5/2,7/2)
0.813 1/2$^+$
0.0 3/2$^+$
^{33}Cl
Pr 67
(p,γ)
l_p
2.981
2.851
1
2.688
3
2.351
(1,2)
1.993
0.812
0
0.0
2
^{33}Cl
Present Work
(d,n)
l_n
2.970
2.937 7/2$^-$
2.869
3
(2)
2.313 3/2$^+$
(2)
1.968 5/2$^{(+)}$
(2)
0.842 1/2$^+$
0
0.0 3/2$^+$
2
^{33}S
En 67

It was considered that a study of the $^{32}S(d,n)^{33}Cl$ reaction with high resolution would be worthwhile from two points of view: to determine precisely the excitation energy of ^{33}Cl levels excited by the (d,n) reaction, and to measure the angular distribution of neutrons to determine the angular momentum, parity and spectroscopic factors of the ^{33}Cl levels.

In the present work, time-of-flight spectra have been taken at three deuteron energies 4.54, 4.70 and 5.50 MeV. The excitation energies of the ^{33}Cl levels have been measured. Angular distributions have been obtained for most of the levels and compared with the Distorted Wave Born approximation and Hauser-Feshbach theories. Absolute spectroscopic factors have been extracted and compared with the shell model predictions.

CHAPTER II

THE EXPERIMENTAL SETUP

2.1 Beam Transport System

To date, the most exact work in neutron spectroscopy has undoubtedly been performed with pulsed accelerators and electronic timing devices to measure the time of flight of neutrons over a certain path length from the target to the detector. Such a technique has the advantages of good energy resolution and applicability to a wide range of neutron energies.

Since in the energy region of interest, the neutron flight times are in the nanosecond region, very short ion bursts of high intensity are needed. To satisfy this requirement both pre-acceleration pulsing and post-acceleration compression have been employed at the University of Alberta 5.5 MeV Van de Graaff. The deuteron beam delivered by the ion source within the high voltage terminal is chopped by means of an RF of 1MHz into pulses of 10 ns duration, which after acceleration are compressed to 0.5 ns duration by means of a Mobley magnet bunching system. A simplified diagram of the beam handling and bunching system together with the Mobley magnet is shown in fig. 2-1. The details of the system have been described previously (Da 66, Gr 67, Mc 67).

Figure 2-1. Beam transport system.

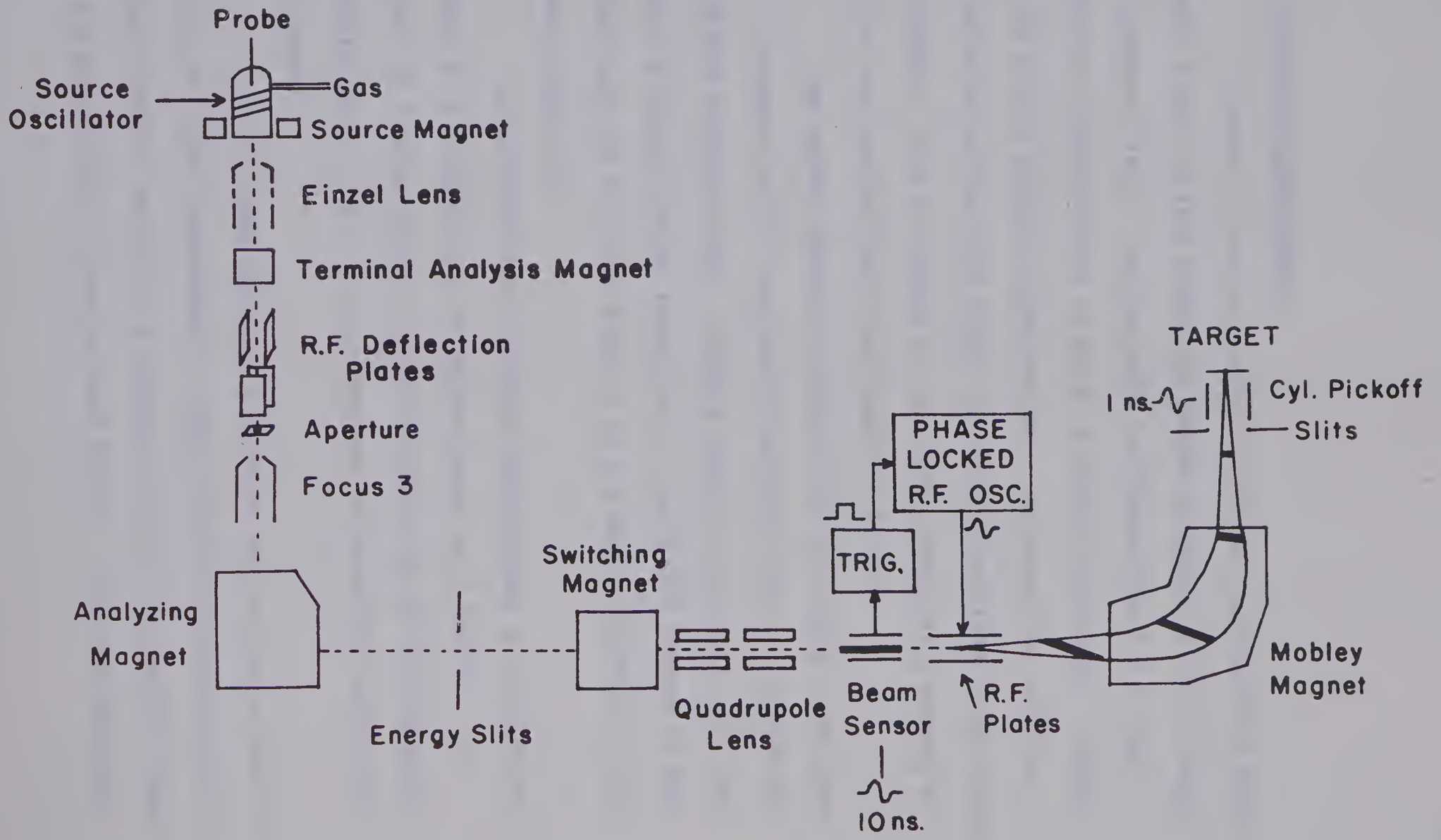
Probe
Source
Oscillator
Gas
Source Magnet
Einzel Lens
Terminal Analysis Magnet
R.F. Deflection
Plates
Aperture
Focus 3
Analyzing
Magnet
Energy Slits
Switching
Magnet
Quadrupole
Lens
PHASE
LOCKED
R.F. OSC.
TRIG.
Beam
Sensor
10 ns.
R.F.
Plates
TARGET
1 ns.
Cyl. Pickoff
Slits
Mobley
Magnet

2.2 The Neutron Spectrometer

In order to time the neutron flight over an accurately known distance, start and stop pulses are needed to operate a Time-to Amplitude Converter (TAC). The stop pulse originates from a 3 cm long cylindrical capacitor which is 30 cm in front of the target. Pulses from the neutron detector start the TAC. The reason for using the detector pulse as the start signal is that the dead time of the system is decreased. This is because the percentage losses is a product of the start rate and the dead time (5μsec) of the TAC.

The neutron detector consists of Ne 218 liquid scintillator in a 3" diameter by 1/2" long quartz container optically coupled to an RCA-4522 photomultiplier. Using a remotely-controlled cart, the detector distance from the target and its angle with respect to the incident beam can be varied from 1.0 to 6.3 meters and from 0 to 150 degrees respectively.

For normalization of angular distributions a fixed-position detector at 2.00 meters and 30 degrees serves as a monitor. It consists of a Naton phosphor optically coupled to an RCA-8575 photomultiplier tube. The monitor system uses the same stop pulse as the main system.

Fig 2-2 shows the block diagram of the electronics used for the time of flight spectrometer. Signals from the photomultiplier of the main detector are fed to a Constant Fraction Pulse Height Trigger (Ge 67) whose output is used to start TAC #1. The signal from the

Figure 2-2. A block diagram of the electronics used for the measurements.

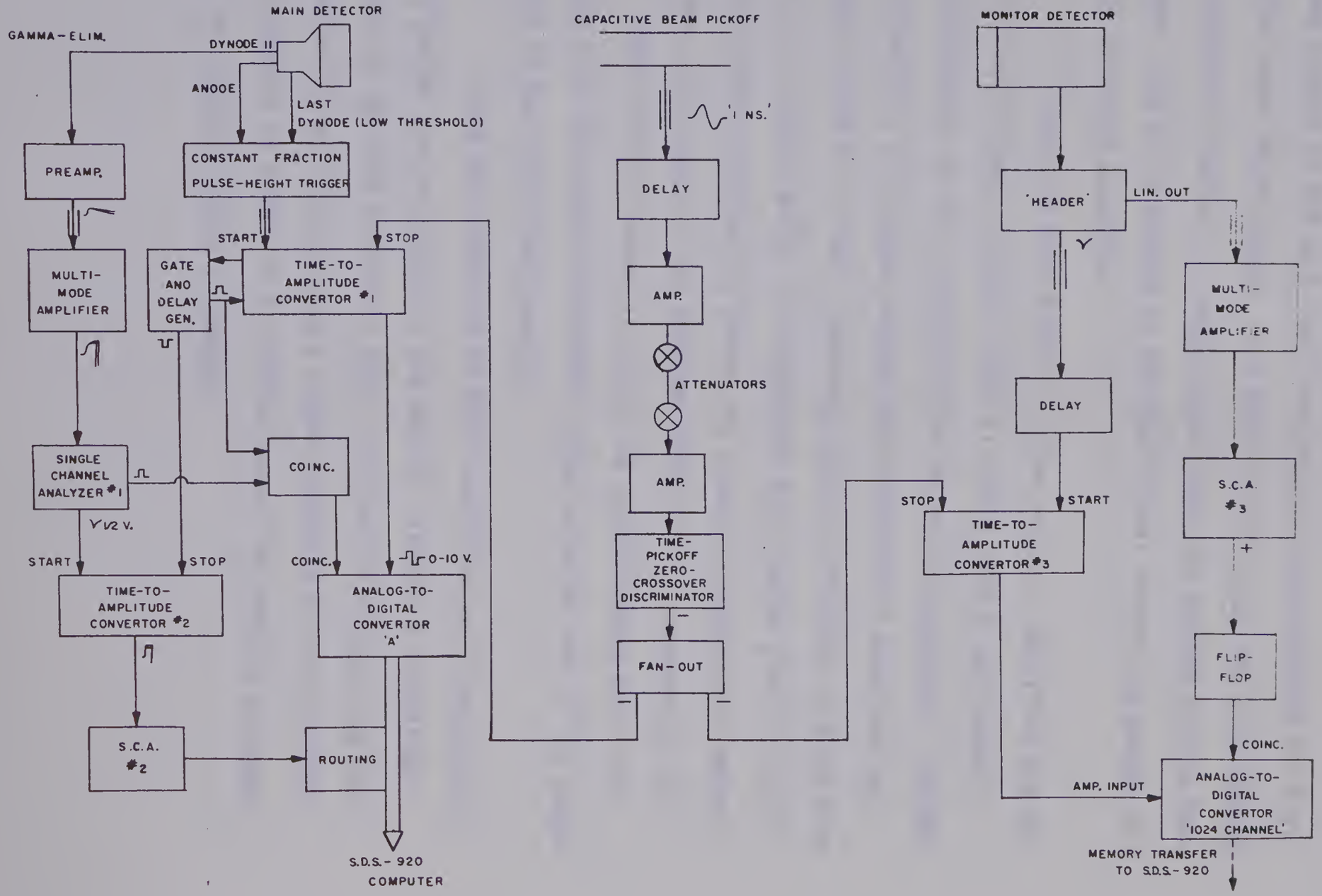
MAIN DETECTOR
GAMMA-ELIM.
DYNODE II
ANOOE
LAST
DYNODE (LOW THRESHOLO)
PREAMP.
CONSTANT FRACTION
PULSE-HEIGHT TRIGGER
MULTI-
MODE
AMPLIFIER
START
STOP
GATE
AND
DELAY
GEN.
TIME-TO-
AMPLITUDE
CONVERTOR #1
SINGLE
CHANNEL
ANALYZER #1
COINC.
+12 V.
START
STOP
COINC.
0-10 V.
TIME-TO-
AMPLITUDE
CONVERTOR #2
ANALOG-TO-
DIGITAL
CONVERTOR
'A'
S.C.A.
#2
ROUTING
S.D.S.-920
COMPUTER
CAPACITIVE BEAM PICKOFF
'1 NS.'
DELAY
AMP.
ATTENUATORS
AMP.
TIME-
PICKOFF
ZERO-
CROSSOVER
DISCRIMINATOR
FAN-OUT
MONITOR DETECTOR
'HEADER'
LIN. OUT
DELAY
MULTI-
MODE
AMPLIFIER
STOP
START
TIME-TO-
AMPLITUDE
CONVERTOR #3
S.C.A.
#3
FLIP-
FLOP
COINC.
AMP. INPUT
ANALOG-TO-
DIGITAL
CONVERTOR
'1024 CHANNEL'
MEMORY TRANSFER
TO S.D.S.-920

beam pickoff is fed to a Fast Zero-Crossover Discriminator (Ge 67a) which stops TAC #1 and #3. The output of TAC #1 is fed to an Analog-to-Digital Converter 'A' (ADCA) which feeds the SDS-920 on-line computer. TAC #1 is strobed by the start signal through the output of a Gate and Delay Generator.

The pulse from dynode 11 (slow pulse) is amplified and fed to a single channel analyzer (SCA) #1, which acts as an integral discriminator, to set a threshold for the neutron detector. The ADCA is gated by a coincidence between the delayed start pulse and the output of SCA #1. Since a gamma-ray pulse is different in shape from that of a neutron pulse, an integration and clipping yields bipolar pulses whose zero-crossing points are timed differently with respect to the leading edge of the detector anode pulse as measured by TAC #2. Using SCA #2 a window is set on the neutron pulses which are routed into the second 2048-channel range while the rest of the pulses remain in the first 2048-channels.

Since the conditions of high resolution and elimination of γ-ray pulses can be relaxed in the monitor circuit, a simplified version of the main circuit is used. In order to decrease the background in the monitor spectrum a higher threshold is set by SCA #3. This spectrum is stored in the '1024-channel' ADC and can be dumped into the computer memory on command.

CHAPTER III

THE EXPERIMENT AND DATA ANALYSIS

3.1 Targets

Elemental sulfur is not a suitable target material since it sublimates in vacuum at room temperature. Several sulfur compounds such as CdS, Ag_2S and Sb_2S_3 have been tried. It has been found that such compounds peel off the backing before they melt. A technique based mainly on the method described by D. D. Watson (Wa 66) has been used to prepare stable targets.

Natural sulfur (95% ^{32}S, 0.76% ^{33}S, 4.22% ^{34}S and 0.02% ^{36}S) has been evaporated in vacuum onto a silver backing. The latter, with the sulfur layer on it, was heated to 200°C in air. An immediate chemical reaction occurs forming a very stable layer of Ag_2S. The advantage of evaporating sulfur in vacuum rather than in air is the better target uniformity. Targets prepared by this method have been proven to be durable and capable of withstanding beam currents of more than 1 μamp at 5.5 MeV for many hours without deterioration. During the experiment air cooling has been applied to these targets.

For absolute normalization of the cross section a gas target has been used. At first H_2S gas was tried as a target but it was found to dissociate under beam bombardment. SO_2 gas has been found to be stable and therefore was used as a target.

3.2 Calibration of the Machine Energy

The machine energy has been calibrated using $Li^7(p,n)^7Be$, $^{13}C(p,n)^{13}N$ and $^{19}F(p,n)^{19}Ne$ thresholds. The estimated error in the calibration is $\leq \pm 5$ KeV.

3.3 Calibration of the Time Spectrum

The time calibration has been done by using the flight time and peak position of the gamma ray group and finding the slope of the calibration line by the electronics setup of fig 3-1. Output pulses from the TAC will occur whenever the start-stop time difference is a multiple integer of the period of the oscillator pulse. By measuring the average spacing of the peaks ($\bar{\Delta}$) in channels, the slope of the time calibration line has been calculated from the relation:

$$\text{Slope} = 10^3/(\bar{\Delta}.f) \text{ ns/channel}$$

where f is the oscillator frequency (mc/sec).

3.4 Detector Efficiency

The neutron detector efficiency was calculated using a computer code developed by T. B. Grandy (Gr 67). The calculations have been compared with detector efficiencies derived from experimental data (Bu 67), and are considered to be accurate to within 8% at the neutron energies encountered in this experiment.

Figure 3-1. Time-Calibration Electronics.

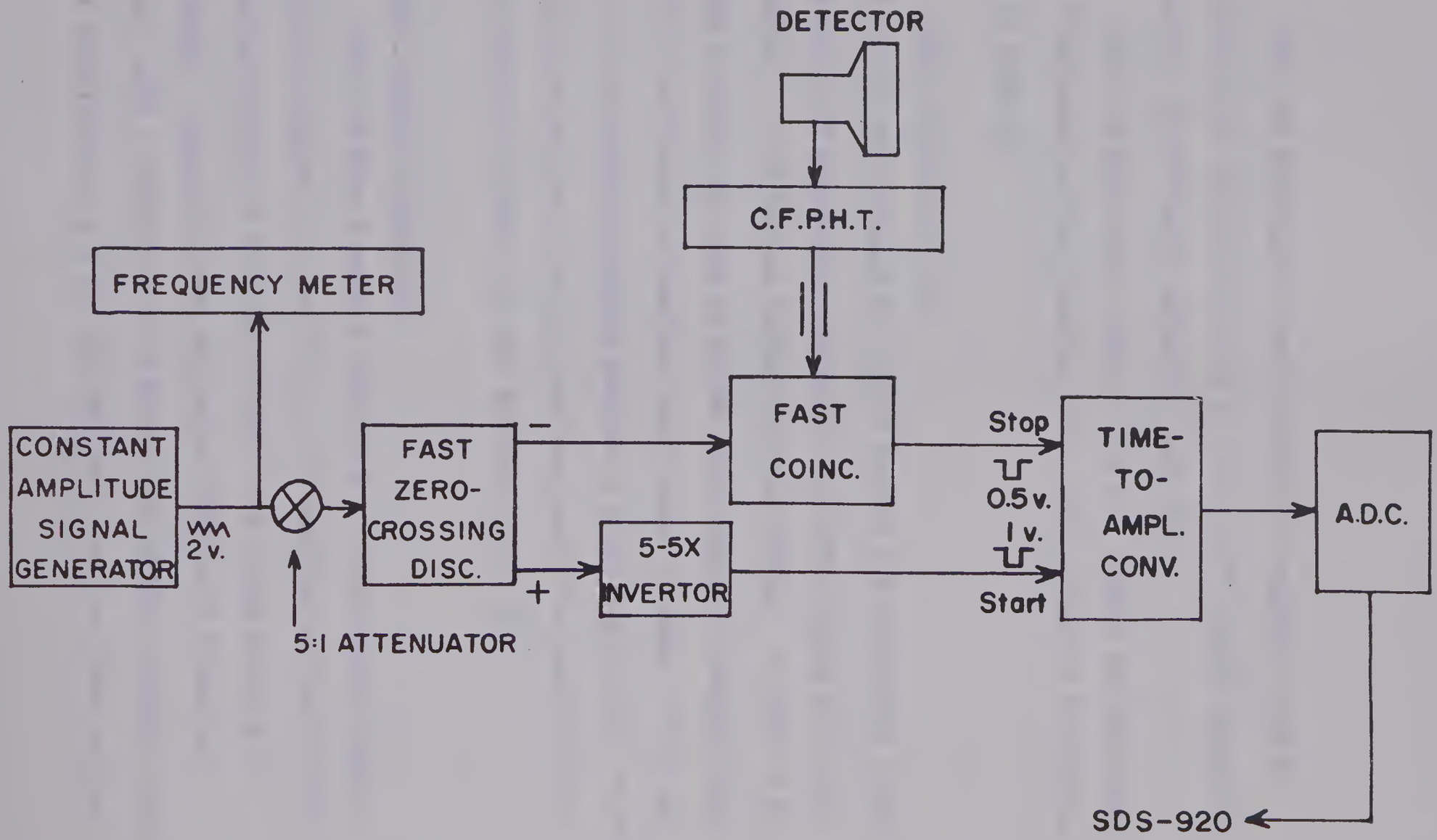
DETECTOR
C.F.P.H.T.
FREQUENCY METER
CONSTANT AMPLITUDE SIGNAL GENERATOR
2 v.
5:1 ATTENUATOR
FAST ZERO-CROSSING DISC.
−
+
5-5X INVERTOR
FAST COINC.
Stop
0.5 v.
1 v.
Start
TIME-TO-AMPL. CONV.
A.D.C.
SDS-920

Since the magnitude of the efficiency is dependent upon the lower threshold as determined by SCA #1, the cutoff neutron energy must be measured. The following method has been used.

Using the electronics setup of fig 3-2, a gamma ray spectrum from a ^{22}Na source has been obtained. The lower threshold in electron energy is given by:

$$\text{Lower threshold} = R.E_c$$

where R is the ratio between the cutoff channel and the channel corresponding to 2/3 of the height of the 0.511 keV Compton edge (fig 3-3). E_c = 340 keV, is the maximum Compton electron energy. In order to get the lower threshold in terms of proton recoil energy, a response curve of Ne 218 scintillator to electrons and protons is needed. Since such a curve is not available, the data published by Smith et al. (Sm 68) for Ne 213, which is quite similar to Ne 218, have been used. The overall error in the detector efficiency has been estimated to be 10%.

3.5 The $^{32}S(d,n)^{33}Cl$ Reaction

Using the beam transport system and the neutron spectrometer (discussed in Chapter II), the $^{32}S(d,n)^{33}Cl$ reaction has been studied at deuteron energies of 4.70 and 5.50 MeV, and flight distance of 6.325 meters. An overall time resolution (FWHM) of 1.2 nsec was obtained. With a flight path of 6.325 m, this implies an energy resolution of 68 keV for the 5.5 MeV neutrons and 15 keV for 2 MeV neutrons.

Figure 3-2. ^{22}Na Gamma ray spectrum.

Figure 3-3. A block diagram of the electronics used for measuring the cut-off neutron energy.

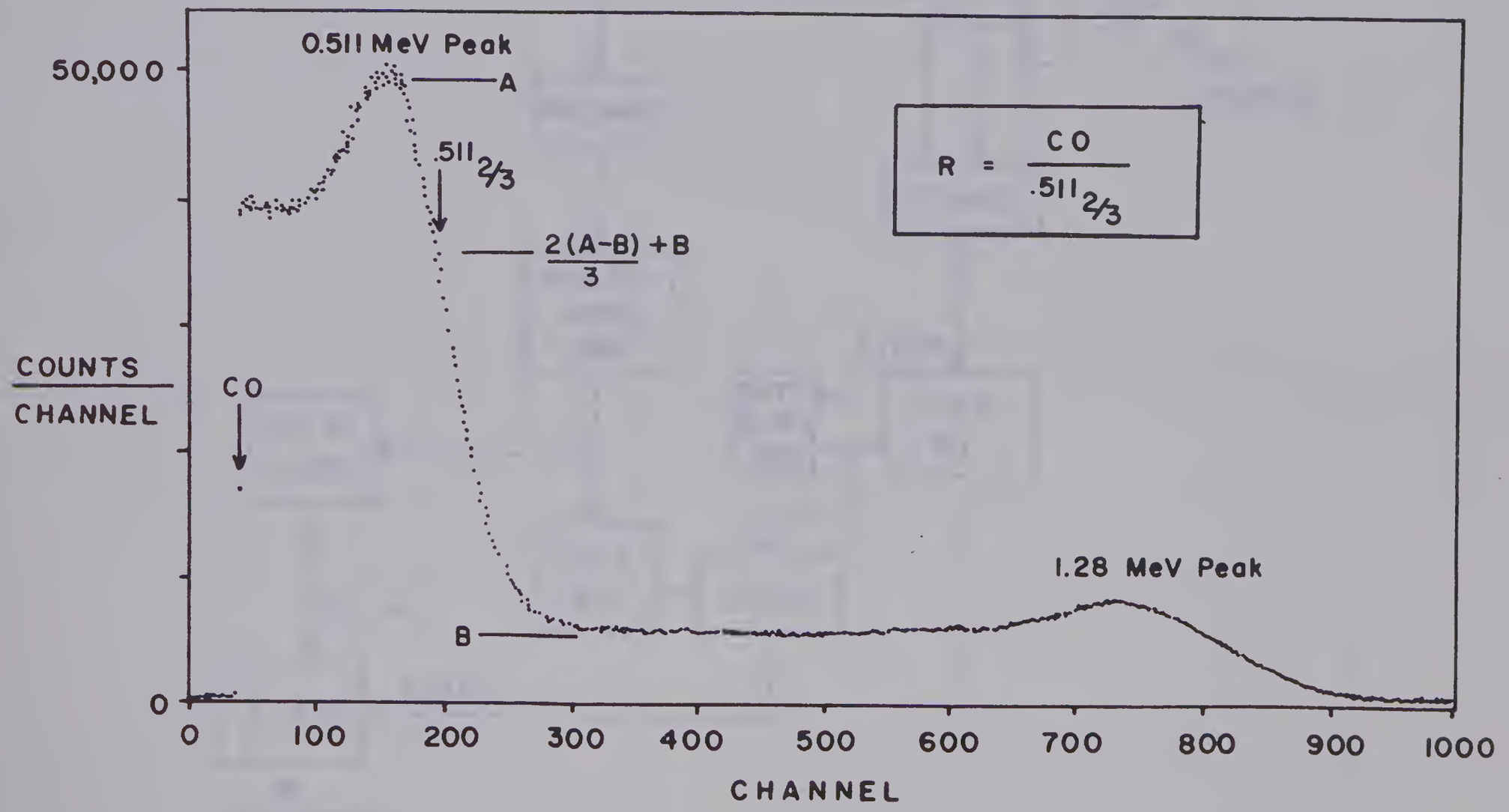
0.511 MeV Peak
A
.511 2/3
2(A-B) +B
3
CO
B
1.28 MeV Peak
R = CO / .511 2/3
50,000
0
COUNTS
CHANNEL
0
100
200
300
400
500
600
700
800
900
1000
CHANNEL

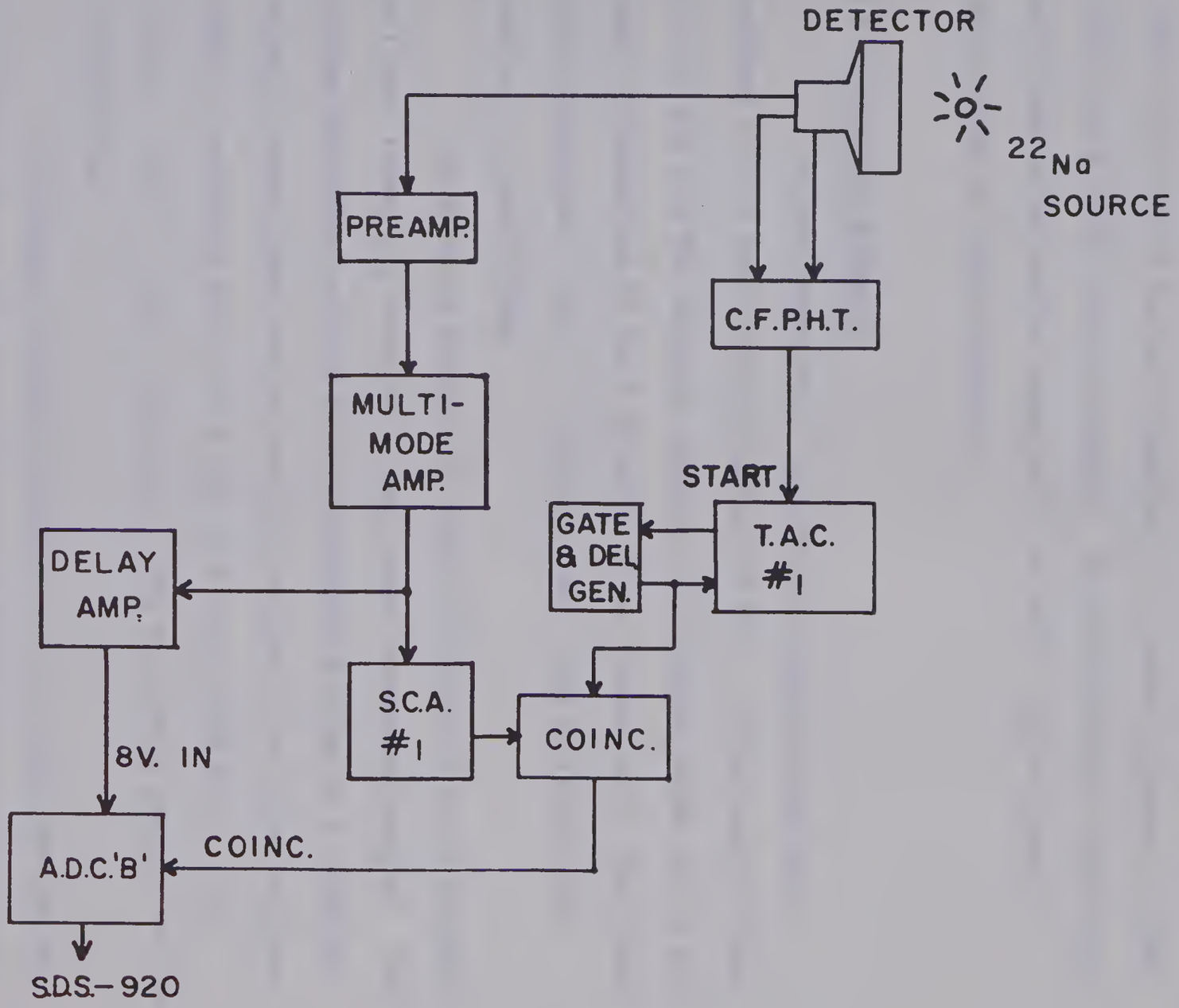
DETECTOR
^{22}Na SOURCE
PREAMP.
C.F.P.H.T.
MULTI-MODE AMP.
START
GATE & DEL GEN.
T.A.C. #1
DELAY AMP.
S.C.A. #1
COINC.
8V. IN
A.D.C.'B'
COINC.
S.D.S.-920

In order to achieve good statistics for the weakly excited levels the reaction has been repeated at a shorter distance of 2.957 meters and 4.54 MeV deuteron energy. In each experiment spectra have been taken in the angular range of 0° to 140°. Fig 3-4 shows a typical time of flight spectrum.

3.6 Excitation Energies

The peak positions of the various neutron groups were obtained using a peak-fitting program (Te 66). For the spectra taken at 4.70 and 5.50 MeV deuteron energies, the program failed to fit the peaks corresponding to the 1.99 and 2.35 MeV states due to their small peak-to-background ratios. Therefore, their peak positions were obtained by hand-fitting.

The deuteron energy, the time calibration line and the peak positions formed the input of a least square mass-and-Q program. This program determines not only the most probable Q-value of a state but the most probable mass for the residual nucleus. The latter was very useful in assigning levels at 1.993, 2.351 and 2.688 MeV to ^{33}Cl nucleus. Table 3-1 shows the output of the mass-and-Q program for the 4.54 MeV data.

The average excitation energies of ^{33}Cl levels derived from all the data of all the runs of the three angular distributions are listed in Table 3-2. These excitation energies are based upon the

Figure 3-4. A neutron time-of-flight spectrum for $^{32}S(d,n)^{33}Cl$ reaction at E_d = 4.70 MeV.

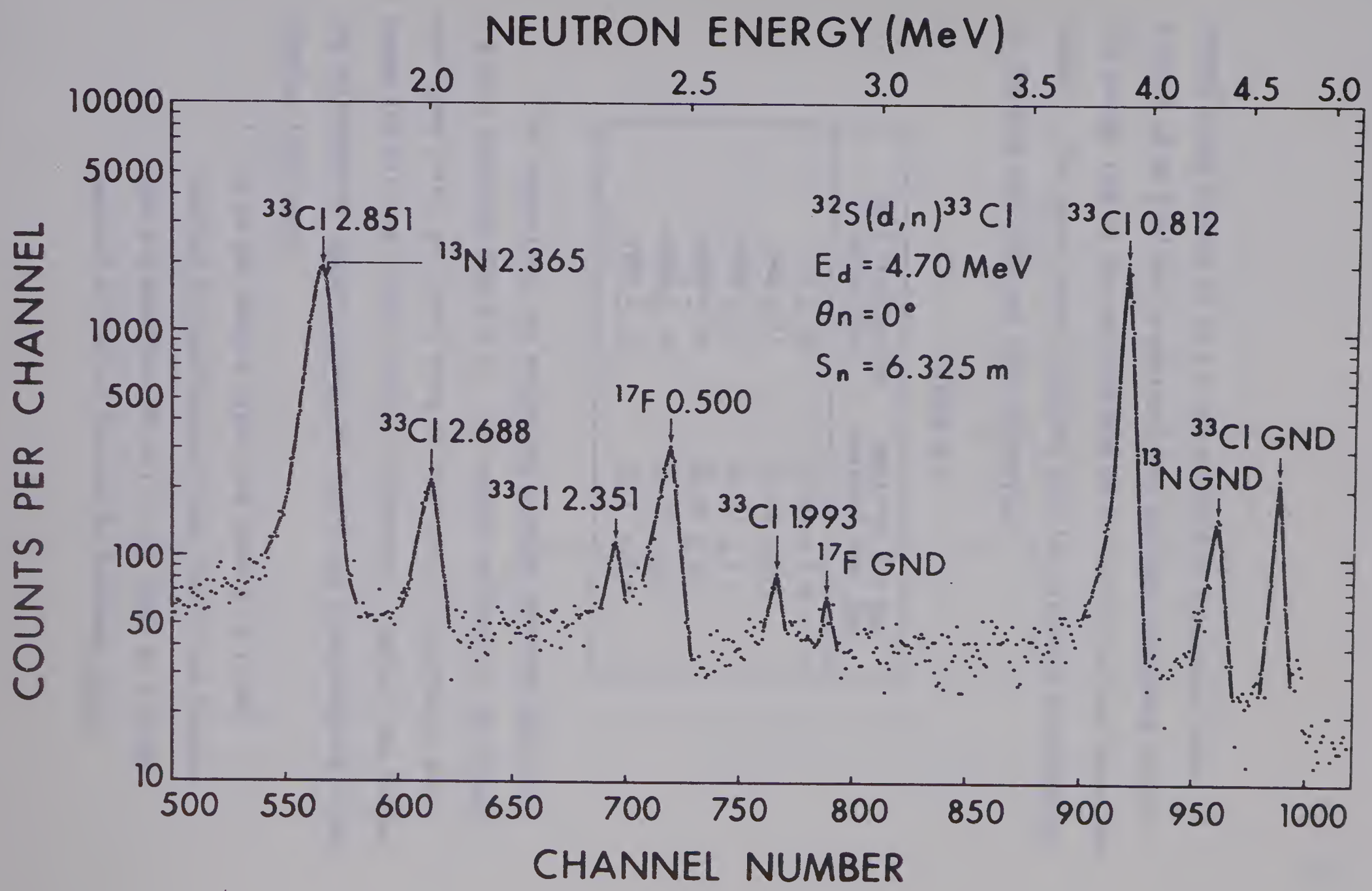
NEUTRON ENERGY (MeV)
2.0
2.5
3.0
3.5
4.0
4.5
5.0
10000
5000
1000
500
100
50
10
COUNTS PER CHANNEL
^{33}Cl 2.851
^{13}N 2.365
^{33}Cl 2.688
^{33}Cl 2.351
^{17}F 0.500
^{33}Cl 1.993
^{17}F GND
^{32}S(d,n)^{33}Cl
E_d = 4.70 MeV
$\theta n = 0°$
S_n = 6.325 m
^{33}Cl 0.812
^{13}N GND
^{33}Cl GND
500
550
600
650
700
750
800
850
900
950
1000
CHANNEL NUMBER

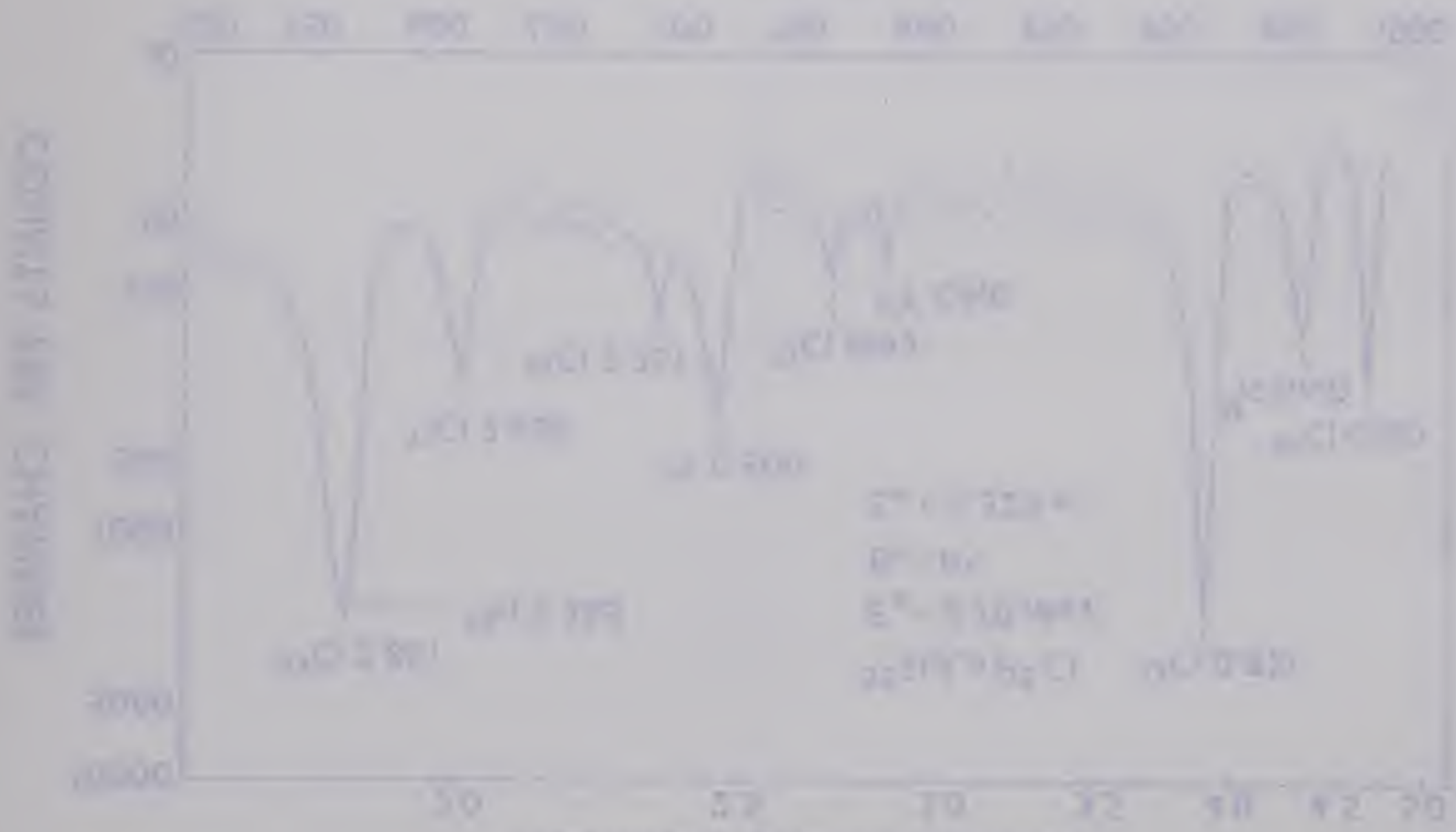

ground state Q-value of 62 ± 9 keV obtained in the present work. A Q-value of 66 ± 12 keV is obtained from the mass difference (En 67). The energy loss of the deuteron beam in the target has been taken into account. The errors were calculated from the estimated uncertainties in the peak positions and time calibration.

TABLE 3-1

Best Fit for the Q-value (keV)	Best Fit for the Residual Mass (MU)
72 ± 16	31.58 ± 1.0
-743 ± 11	31.49 ± 0.9
-1936 ± 11	32.24 ± 1.0
-2304 ± 8	32.25 ± 0.9
-2636 ± 4	31.87 ± 0.6
-2799 ± 3	32.11 ± 0.6

For comparison, the excitation energies obtained previously are also tabulated (Table 3-2). The results obtained in the present work agree fairly well with those of Moss (Mo 67) and Prosser and Gordon (Pr 67) from (^{3}He,d) and (p,γ) reactions. However, the following discrepencies appear between our results and those obtained in the previous (d,n) work:

(i) We do not observe either the state at 2.11 MeV reported by Macefield and Towle (Ma 60) and Mubarakmand and Macefield (Mu 67) or the level at 2.53 MeV reported by both of them and by Middleton *et al*.

TABLE 3-2

Q-value (KeV)	EXCITATION ENERGY (KeV)					
Present Work	Present Work	Mi 53 (d,n)	Ma 60 (d,n)	Gr 66 (^{3}He,d)	Mo 67 (^{3}He,d)	Pr 67 (P,γ)
62 ± 9	g.s.	g.s.	g.s.	g.s.	g.s.	g.s.
-750 ± 9	812 ± 4	760 ± 70	880 ± 70	816 ± 8	810 ± 9	813 ± 4
-1931 ± 11	1993 ± 6	(1890)[b]			(1999 ± 20)[c]	1990 ± 4
			2110 ± 60			
-2289 ± 10	2351 ± 5				2351 ± 9	2347 ± 10
			2530 ± 60			
-2626 ± 9	2688 ± 4			2675 ± 4	2686 ± 9	(2686)[d]
-2789 ± 9	2851 ± 4	2840 ± 60	2820 ± 60	2835 ± 4	2848 ± 9	2847 ± 20 2855 ± 20
(-2918 ± 17)[a]	(2980 ± 12)[a]					2979 ± 4

a--A rather weak neutron group was observed in the spectra taken at backward angles.

b--A weak indication for a peak was observed at certain angles.

c--The excitation energy of this level is obtained from $^{36}Ar(p,\alpha)^{33}Cl$ reaction.

d--The excitation energy is that of Mo 67.

(Mi 53). On the other hand we do observe states at 1.993, 2.351 and 2.688 MeV which they did not see except for a weak level at 1.98 MeV reported by Middleton et al.

(ii) In Grandy et al. (Gr 68) experiment on a ^{42}Ca target which was contaminated with ^{32}S, levels at 2.12, 2.56, 2.63 and 2.69 MeV have been identified. Only the 2.69 MeV state has been confirmed in the present experiment. Comparing the peak-to-background ratio of the spectra obtained in the present work and that of Grandy et al., it is found that they are the same. Thus the extra peaks observed by Grandy et al. must have been due to some unknown contaminant other than ^{32}S.

3.7 Cross Sections

Using plot-and-print program (Da 69) the background in the raw spectra was calculated using a parabolic shape. Peak areas of the various neutron groups were extracted. However, in the 5.5 MeV data, the areas of the 1.99 MeV and 2.35 MeV peaks could not be obtained due to the small peak-to-background ratio. Hand-fitting has been used to obtain the areas of these peaks in the 4.54 and 4.70 MeV data.

The neutrons which are misidentified as gamma rays appear as peaks in the gamma ray spectrum. These peaks were summed and added

to the corresponding areas in the neutron part of the spectrum.

The contaminant peaks due to the presence of ^{12}C and ^{16}O, which interfere with those of ^{33}Cl at certain angles, were subtracted. The results of N. Davison (Da 68) on ^{17}F states and those of A. W. Obst (Ob 66) and C. E. Hollandsworth et al. (Ho 66) on ^{13}N states have been used for this purpose.

The peak areas obtained were normalized to the area of the ground state peak of ^{33}Cl in the monitor spectrum.

The relative corrected areas were calculated using the formula:--

$$\text{Relative Corrected Area} = \frac{A+A_\gamma}{A_m} \cdot \frac{t_m}{t} \cdot \frac{1}{\varepsilon}$$

where A = area of the neutron peak in the neutron spectrum

A_γ = area of the corresponding neutron peak in the gamma spectrum

t_m = monitor system live time

t = main detector live time

ε = absolute efficiency of the neutron detector

For the data taken at 4.54 and 4.70 MeV deuteron energy the absolute normalization of cross sections has been carried out using a gas target. At first the $D(d,n)^3He$ experiment was done to check the charge collection in the gas cell. A value of 67.5 $\pm$ 7 mb/sr was

obtained for the cross section at 0° and 4.50 MeV deuteron energy. This value agrees fairly well with the published value of 72.0 ± 5 mb/sr at a deuteron energy of 4.60 MeV (St 56).

A run at 0° with SO_2 gas at a pressure of 16.45 mm Hg was used to calculate the absolute differential cross section. The area of the 0.81 MeV peak was extracted and corrected for dead time. The corresponding absolute differential cross section was calculated using the formula:

$$(d\sigma/d\Omega) = 1.6 \times 10^{14} \cdot (A/QN\Omega\varepsilon) \qquad \text{mb/sr}$$

A = area of the peak after corrections for detector dead time have been made

Q = charge collected (μC)

N = number of ^{32}S nuclei/cm^2 present in the gas cell

Ω = solid angle subtended by the detector = 1.51×10^{-4} sr at 6.3 meters

ε = absolute efficiency of the neutron detector

As a second check on the absolute cross sections the target thickness has been measured independently by determining the energy width at half maximum of the 2.69 MeV peak. The results of this method agree to within 5% with that of the gas target method. For the 5.5 MeV runs, the absolute normalization has been done using the energy width method.

The absolute cross sections for the states of ^{33}Cl are given

in Tables 3-3 to 3-8.

The errors noted are those due to counting statistics. These errors are quite large for the 1.99 MeV state due to the small peak-to-background ratio. The imperfect extraction of the 2.35 MeV peak from that of $^{17}F_{0.5}$ was the major source of error in the cross sections of this state. Not shown are the errors arising from the detector efficiency (10%) and the absolute normalization (11%). Thus the absolute cross sections will have an additional error of 15%.

DIFFERENTIAL CROSS SECTION FOR THE GROUND STATE

E_d = 4.70 MeV			E_d = 5.50 MeV		
c.m. Angle deg.	$(d\sigma/d\Omega)_{c.m.}$ mb/sr	Error mb/sr	c.m. Angle deg.	$(d\sigma/d\Omega)_{c.m.}$ mb/sr	Error mb/sr
0.0	1.98	0.07	0.0	0.83	0.06
5.2	1.97	0.10	5.2	1.00	0.07
10.4	2.47	0.08	10.4	1.49	0.06
15.7	3.01	0.13	20.9	2.66	0.11
20.9	3.65	0.10	31.3	4.10	0.14
31.3	4.46	0.13	41.6	3.77	0.12
41.6	3.74	0.10	51.9	2.86	0.12
51.9	2.36	0.08	62.2	1.53	0.06
62.2	1.16	0.05	72.4	1.01	0.05
72.4	1.22	0.06	82.5	1.01	0.07
82.5	1.25	0.05	92.5	1.07	0.04
102.5	1.53	0.05	112.4	1.07	0.07
122.2	1.40	0.04	131.9	0.82	0.06
141.6	1.20	0.04	143.4	0.72	0.09

TABLE 3-3

DIFFERENTIAL CROSS SECTION FOR THE 0.812 MeV STATE

E_d = 4.70 MeV			E_d = 5.50 MeV		
c.m. Angle deg.	$(d\sigma/d\Omega)_{c.m.}$ mb/sr	Error mb/sr	c.m. Angle deg.	$(d\sigma/d\Omega)_{c.m.}$ mb/sr	Error mb/sr
0.0	23.59	0.52	0.0	25.04	0.90
5.2	21.90	0.49	5.2	22.84	0.82
10.5	16.63	0.37	10.5	16.18	0.58
15.8	9.22	0.26	20.9	4.48	0.16
21.0	6.27	0.17	31.4	0.28	0.02
31.4	1.38	0.07	41.8	0.89	0.07
41.8	1.57	0.07	52.1	2.07	0.08
52.1	2.85	0.10	62.4	2.71	0.07
62.4	2.71	0.07	82.7	1.20	0.08
72.6	2.49	0.09	92.7	0.49	0.02
82.7	1.73	0.05	112.6	0.26	0.03
102.7	0.85	0.03	132.1	0.50	0.06
122.4	0.78	0.23	143.5	0.78	0.05
141.8	1.11	0.03			

TABLE 3-4

DIFFERENTIAL CROSS SECTION FOR THE 1.993 MeV STATE

E_d = 4.54 MeV			E_d = 4.70 MeV		
c.m. Angle deg.	$(d\sigma/d\Omega)_{c.m.}$ mb/sr	Error mb/sr	c.m. Angle deg.	$(d\sigma/d\Omega)_{c.m.}$ mb/sr	Error mb/sr
0.0	0.52	0.05	0.0	0.53	0.08
5.3	0.55	0.06	5.3	0.54	0.07
10.6	0.60	0.05	10.6	0.64	0.08
15.9	0.63	0.05	15.9	0.39	0.06
21.2	0.64	0.06	21.2	0.56	0.10
26.4	0.62	0.07	31.7	0.57	0.11
31.7	0.52	0.06	42.2	0.58	0.09
37.0	0.48	0.06	52.6	0.62	0.08
42.2	0.40	0.05	73.2	0.46	0.08
52.6	0.40	0.04	83.3	0.41	0.06
63.0	0.35	0.04	103.4	0.39	0.03
83.4	0.51	0.05	123.0	0.38	0.03
103.4	0.34	0.04	142.2	0.38	0.05
123.0	0.47	0.04			

TABLE 3-5

DIFFERENTIAL CROSS SECTION FOR THE 2.351 MeV STATE

E_d = 4.54 MeV			E_d = 4.70 MeV		
c.m. Angle deg.	$(d\sigma/d\Omega)_{c.m.}$ mb/sr	Error mb/sr	c.m. Angle deg.	$(d\sigma/d\Omega)_{c.m.}$ mb/sr	Error mb/sr
0.0	0.70	0.10	0.0	0.50	0.08
5.3	0.72	0.07	5.3	0.59	0.09
10.6	0.97	0.07	10.6	0.73	0.09
16.0	0.97	0.06	~~15.9~~	~~0.47~~	~~0.05~~
21.3	1.06	0.08	21.2	0.~~1~~6 0.82	0.02
26.6	1.22	0.07	31.8	0.87	0.12
31.9	1.16	0.09	42.3	0.92	0.09
37.1	0.94	0.06	52.8	0.68	0.09
42.4	0.82	0.05	63.1	0.34	0.07
52.8	0.27	0.02	73.4	0.27	0.06
63.2	0.21	0.01	83.6	0.17	0.04
83.6	0.43	0.06	103.6	0.30	0.04
103.6	0.41	0.05	123.1	0.43	0.04
123.2	0.26	0.03	142.3	0.42	0.06
142.4	0.16	0.04			

TABLE 3-6

DIFFERENTIAL CROSS SECTION FOR THE 2.688 MeV STATE

E_d = 4.70 MeV			E_d = 5.50 MeV		
c.m. Angle deg.	$(d\sigma/d\Omega)_{c.m.}$ mb/sr	Error mb/sr	c.m. Angle deg.	$(d\sigma/d\Omega)_{c.m.}$ mb/sr	Error mb/sr
0.00	2.67	0.07	0.0	3.82	0.17
5.3	2.57	0.07	5.3	3.73	0.13
10.7	2.89	0.08	10.6	3.64	0.16
16.0	2.07	0.11	21.2	3.41	0.15
21.4	2.52	0.11	31.8	3.41	0.15
32.0	2.92	0.11	42.3	3.11	0.10
42.6	2.88	0.10	52.8	3.04	0.13
53.0	2.85	0.10	63.1	2.45	0.08
63.4	2.62	0.07	73.4	2.15	0.09
73.7	2.33	0.08	83.5	1.79	0.11
83.9	1.96	0.04	93.6	1.65	0.03
103.9	1.81	0.04	113.4	1.67	0.07
123.4	1.50	0.05	132.8	1.01	0.04
142.5	1.15	0.03	144.0	0.79	0.08

TABLE 3-7

DIFFERENTIAL CROSS SECTION FOR THE 2.851 MeV STATE

E_d = 4.70 MeV			E_d = 5.50 MeV		
c.m. Angle deg.	$(d\sigma/d\Omega)_{c.m.}$ mb/sr	Error mb/sr	c.m. Angle deg.	$(d\sigma/d\Omega)_{c.m.}$ mb/sr	Error mb/sr
0.0	33.15	0.74	0.0	40.10	1.44
5.4	32.41	0.72	5.3	39.36	1.41
10.7	34.75	0.77	10.6	39.25	1.41
16.1	21.36	0.47	21.3	35.88	1.29
21.4	23.02	0.51	31.9	26.04	0.93
32.1	24.56	0.61	42.4	12.66	0.42
42.7	17.39	0.38	52.8	8.09	0.34
53.2	11.70	0.26	63.2	6.48	0.27
63.6	7.25	0.16	73.5	6.18	0.25
73.9	7.72	0.17	83.66	5.56	0.23
84.1	6.90	0.12	93.7	5.62	0.23
104.1	5.91	0.10	113.5	4.03	0.16
123.6	4.50	0.11	132.8	3.31	0.17
142.7	4.10	0.10	144.1	3.35	0.17

TABLE 3-8

CHAPTER IV

THEORETICAL ANALYSIS OF ANGULAR DISTRIBUTIONS

4.1 Background

The two main mechanisms through which a nuclear reaction can proceed are the compound nucleus (CN) and the direct modes. Both may simultaneously contribute to the measured reaction cross section. Therefore, to analyze the direct part, the CN contribution should be subtracted from the experimental cross section.

Using a statistical approach Hauser and Feshbach (Ha 52) have obtained an analytic expression for the differential cross section of a reaction when it proceeds via CN mode. Their method is known as Hauser-Feshbach (HF) theory.

Direct reactions have been successfully explained by the Distorted Wave Born Approximation theory (DWBA). It refers to the method of calculating the differential cross section of stripping using the optical model wave functions. A detailed mathematical treatment of the DWBA theory has been developed by a number of authors. Excellent among these are those given by Tobocman (To 61) and G. R. Satchler (Sa 64).

The greatest significance of the analysis of the direct part is that it can yield the orbital angular momentum l of the captured particle. The following model-independent selection rules can

be used to determine the change of angular momentum and parity in a stripping process:

$$|(|J_i - J_f| - \tfrac{1}{2}| \leq J_f < J_i + l + \tfrac{1}{2}$$

$$\pi_i \pi_f = (-1)^l$$

where J_i, J_f, π_i and π_f are the initial and final spins and parities. If the spin of the target nucleus is 0^+, the final state will have spin $J_f = l \pm \frac{1}{2}$ and parity $= (-1)^l$.

The l-value of the captured particle is obtained from fitting the direct part of the experimental angular distribution with the DWBA predictions. In doing so, the ordinates of the theoretical curves have to be adjusted so as to make them match the data at the principal maximum. The DWBA calculations are based on the assumption that the captured particle goes into a single-particle state, i.e., a shell model state. If this is not the case, the experimental cross-section, of course, will be lower than the calculated one. In general, one can write:

$$(d\sigma/d\Omega)_{exp} = S(d\sigma/d\Omega)_{th}$$

where the factor S, called the spectroscopic factor, measures the ratio of the observed cross section to the cross section expected for a single-particle state. Put differently, it measures the percentage contribution of a single-particle state or states with a given angular

momentum l to the total wave function describing the residual state.

4.2 Analysis of Angular Distributions

For the reaction studied in this thesis a program written by W. R. Smith (Sm 65) and modified by N. Davison (Da 68) to include the level density formulae has been used to calculate the CN contribution. The resultant CN cross sections for the (d,n) channel were found to be too small (fig. 4-3) to affect the experimental cross sections for any level of ^{33}Cl. This can be attributed to the high level density in the (d,p) channel.

As a result, the experimental angular distributions were only compared to the DWBA predictions. A DWBA code written by P. D. Kunz (Ku 67) was used to calculate the $^{32}S(d,n)^{33}Cl$ differential cross sections. For the entrance and exit channels, optical potentials of the type:

$$U(r) = U_c(r) - V\, f(r,r_{or},a_r) + 4ia_i\, W \frac{d}{dr}[f(r,r_{oi},a_i)] + \frac{\hbar^2}{m_\pi c}\, V_s \frac{1}{r}\frac{d}{dr}[f(r,r_{os},a_s)]\, \vec{L}\cdot\vec{\sigma}$$

were used, where the Coulomb potential U_c is that of a uniformly charged sphere of radius

$$R_c = r_{oc} A^{\frac{1}{3}}$$

The form factors for the other potentials are taken to have the Saxon-Woods shape

$$f(r,r_o,a) = \{1 + \exp [(r - r_o A^{\frac{1}{3}})/a]\}^{-1}$$

V, r_o and a are the strength, radius and diffussness of the potential. The subscripts r, i and s refer to the real, imaginary and spin-orbit potentials, respectively. The wave function of the captured proton was obtained by solving Schrodinger equation with the potential

$$U_p(r) = U_c(r) - V \{f(r,r_{or},a_r) - \lambda_{so} (\hbar/2m_p c)^2 \frac{1}{r} \frac{d}{dr} [f(r,r_{os},a_s)] \vec{L} \cdot \vec{\sigma}\}$$

where λ_{so} determines the strength of the spin-orbit potential. For a given binding energy, the computer code adjusts V until the solution gives the same binding energy.

The code DWUCK containes the options for finite range effect and non-locality of potentials. The first is approximated by incorporating in the zero range approximation the radial correction factor:

$$\Lambda(r) = \{1 + R^2(2m_p m_n/\hbar^2 m_d) (U_d(r) - U_p(r) - B_d)\}^{-1}$$

where m_d, m_p and m_n are the masses of the deuteron, proton and neutron respectively, and B_d is the binding energy of the deuteron. R is the finite range parameter. The non-locality of the potentials is taken into account by multiplying the wave

functions generated by the equivalent local potentials by factors of the form:

$$F(r) = \{1 - \beta^2(m/2\hbar^2)U(r)\}^{-\frac{1}{2}}$$

where β is the non-locality parameter.

The initial deuteron optical model parameter used were those obtained by Perey and Perey (Pe 66) from the elastic scattering of 11.8 MeV deuterons on natural sulfur. Since these parameters are obtained at considerably higher energy than that at which the present work was carried out, the depth of the imaginary well has been decreased to reduce the probability of absorption of the deuteron by the target nucleus.

Neutron parameters for the outgoing channel are those of Perey and Buck as compiled by Rosen (Ro 66).

Table 4-1 gives the optical model parameters used in both HF and DWBA calculations.

Figures 4-1 to 4-6 show the experimental data and the DWBA predictions for the differential cross section for ^{33}Cl levels. The DWBA predictions were calculated with local potentials ($\beta = 0$), a lower cutoff of zero fm in the radial integral and a value of R = 0.621 fm for finite range correction.

OPTICAL MODEL PARAMETERS USED IN DWBA AND HF CALCULATIONS

Parameter	Deuteron[a]	Deuteron[b]	Captured Proton	Neutron	Proton[c]	Alpha[c]
V(MeV)	154.6	154.6	Adjusted by the computer code	47.0	54.1	200.0
r_{or}(fm)	0.785	0.785	1.25	1.27	1.25	1.69
a_r(fm)	0.953	0.953	0.65	0.86	0.65	0.576
W(MeV)	14.6	9.0		9.6	13.5	9.0
r_{oi}(fm)	1.567	1.567		1.27	1.25	1.69
a_i(fm)	0.534	0.534		0.47	0.47	0.576
V_s(MeV)	5.91	5.91		7.2	7.5	0.0
r_{os}(fm)		0.785	1.25	1.27		
a_s(fm)		0.953	0.65	0.66		
r_{oc}(fm)		1.3	1.25			
λ_{so}			28			

(a) Optical Model Parameters of Perey and Perey (Pe 66).

(b) Optical Model Parameters used in the present work.

(c) The proton and alpha particle optical model parameters were used only in the Hauser-Feshbach Calculation.

TABLE 4-1

Figure 4-1. Angular distribution of the neutrons leading the ground state of ^{33}Cl for E_d=4.70 and 5.50 MeV. The error bars indicate the statistical errors. The solid curves are the DWBA predictions.

Figure 4-2. Angular distribution of the neutrons leading to the 0.812 MeV state of ^{33}Cl for E_d=4.70 and 5.50 MeV (see also caption under figure 4-1.

Figure 4-3. Angular distributions of the neutrons leading to the 1.993 MeV state of ^{33}Cl for E_d=4.54 and 4.70 MeV. The dashed curve is the predictions of the HF calculations for E_d=4.54 assuming $J^{\pi}=5/2^{+}$.

Figure 4-4. Angular distribution of the neutrons leading to the 2.351 MeV state of ^{33}Cl for E_d=4.54 and 4.70 MeV (see also caption under figure 4-1).

Figure 4-5. Angular distribution of the neutrons leading to the 2.688 MeV state of ^{33}Cl for E_d=4.70 and 5.50 MeV (see also caption under figure 4-1).

Figure 4-6. Angular distribution of neutrons leading to the 2.851 MeV state of ^{33}Cl for E_d=4.70 and 5.50 MeV. Points without error bars indicate that the errors are $\leq$ the size of the points (see also caption under figure 4-1).

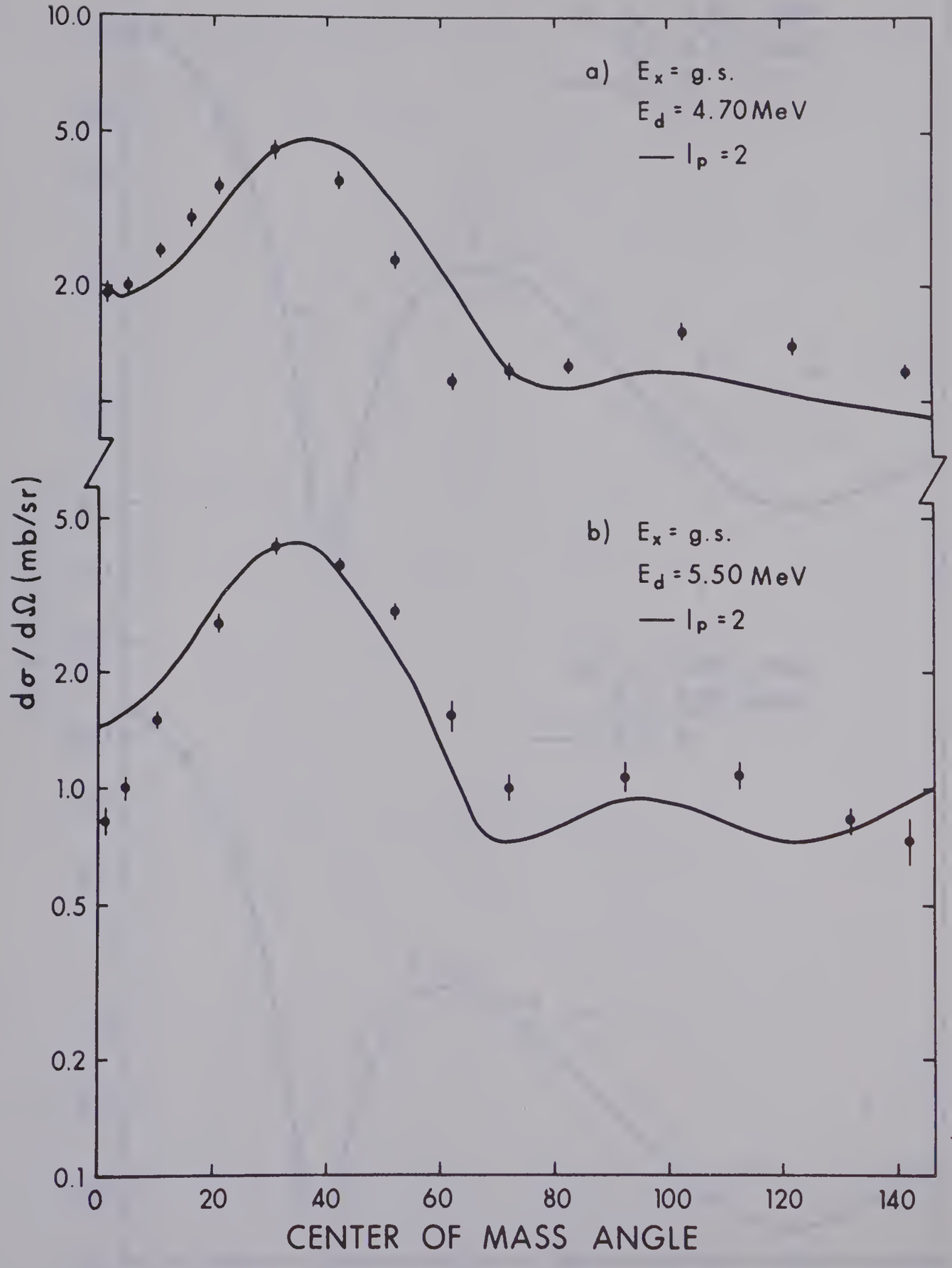
a) E_x = g.s.
E_d = 4.70 MeV
— l_p = 2
b) E_x = g.s.
E_d = 5.50 MeV
— l_p = 2
dσ / dΩ (mb/sr)
10.0
5.0
2.0
1.0
0.5
0.2
0.1
0
20
40
60
80
100
120
140
CENTER OF MASS ANGLE

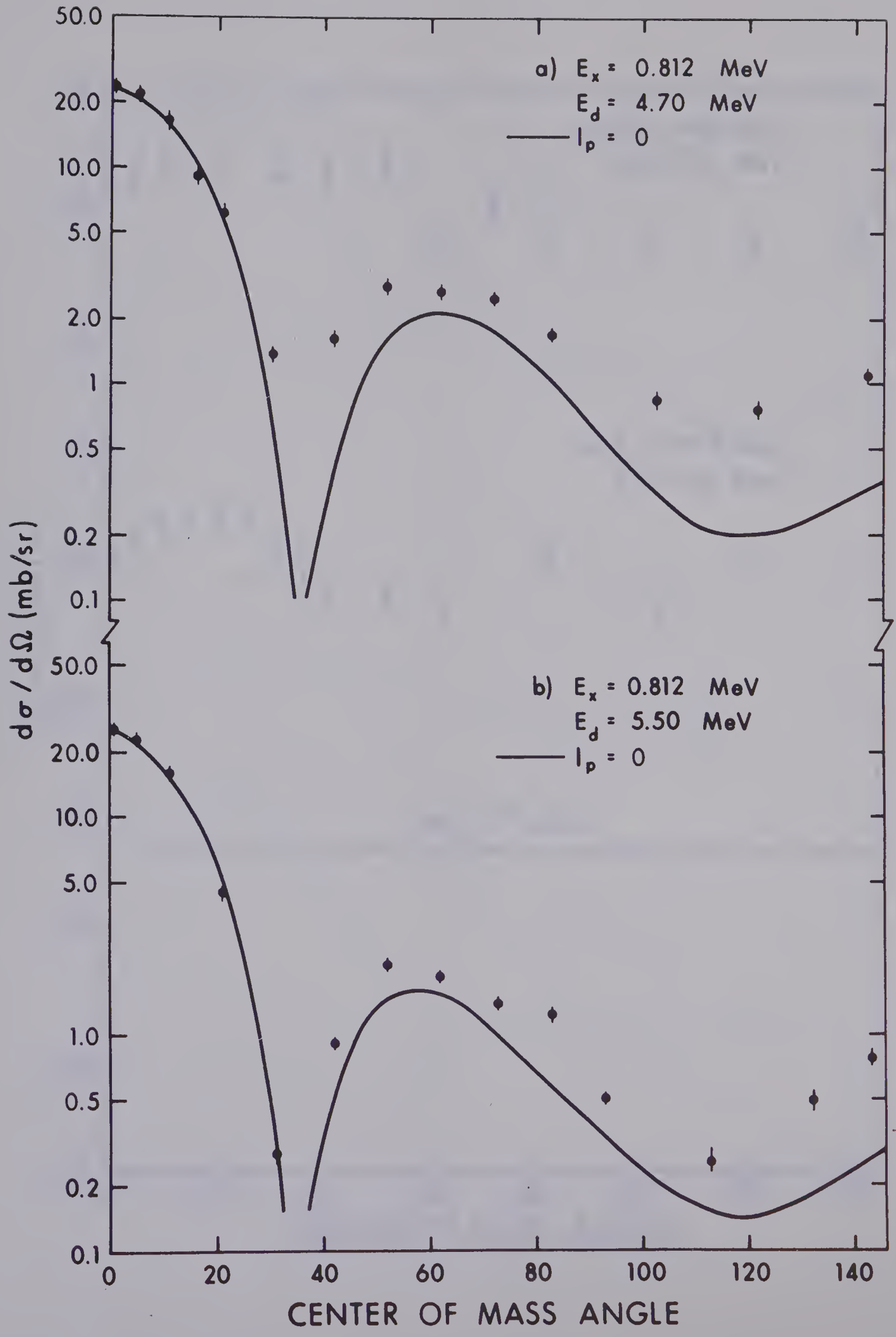
a) E_x = 0.812 MeV
E_d = 4.70 MeV
l_p = 0
b) E_x = 0.812 MeV
E_d = 5.50 MeV
l_p = 0
dσ / dΩ (mb/sr)
CENTER OF MASS ANGLE
50.0
20.0
10.0
5.0
2.0
1
0.5
0.2
0.1
1.0
0
20
40
60
80
100
120
140

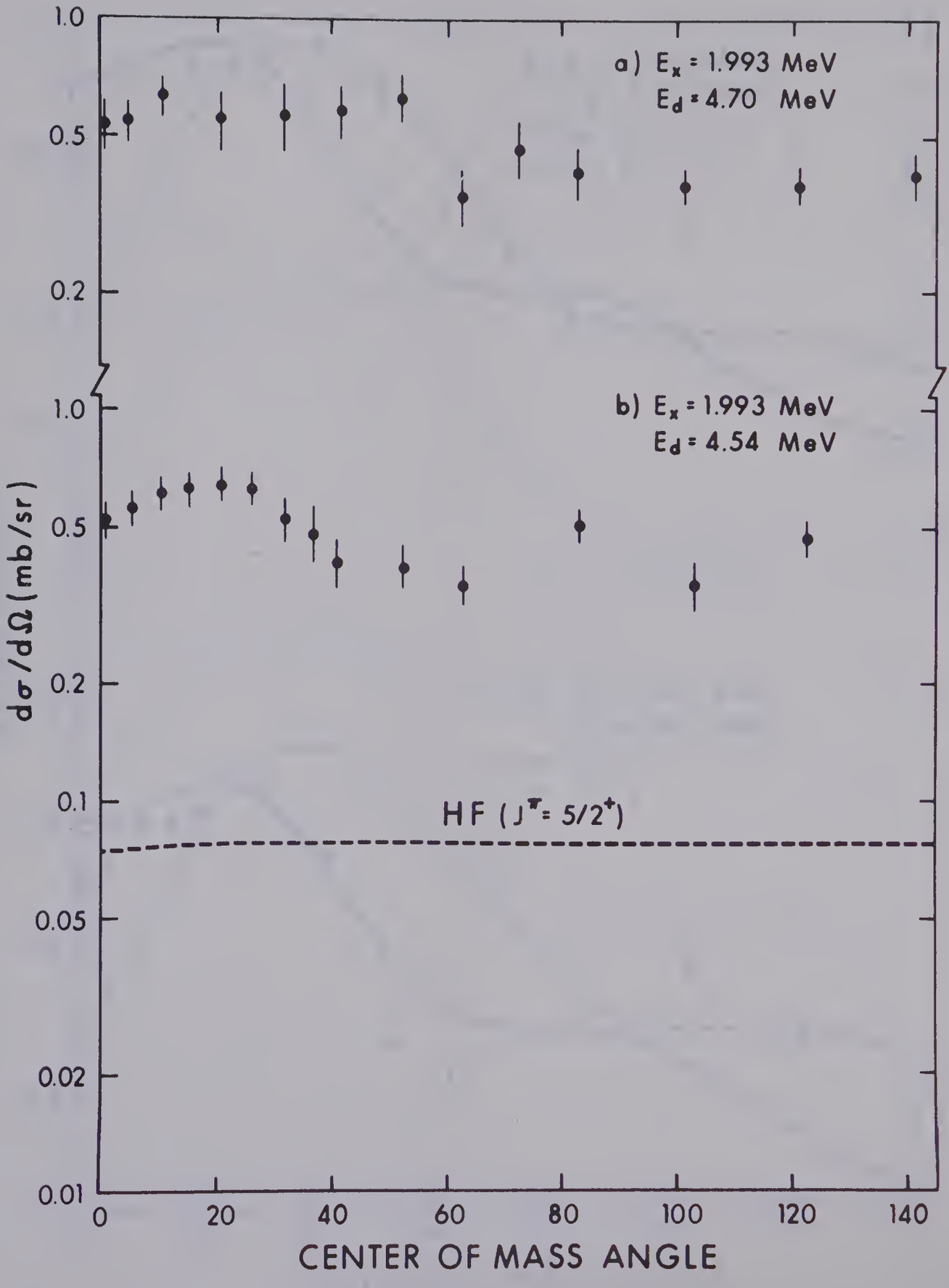
a) E_x = 1.993 MeV
E_d = 4.70 MeV
b) E_x = 1.993 MeV
E_d = 4.54 MeV
HF ($J^\pi = 5/2^+$)
$d\sigma/d\Omega$ (mb/sr)
CENTER OF MASS ANGLE
1.0
0.5
0.2
0.1
0.05
0.02
0.01
0
20
40
60
80
100
120
140

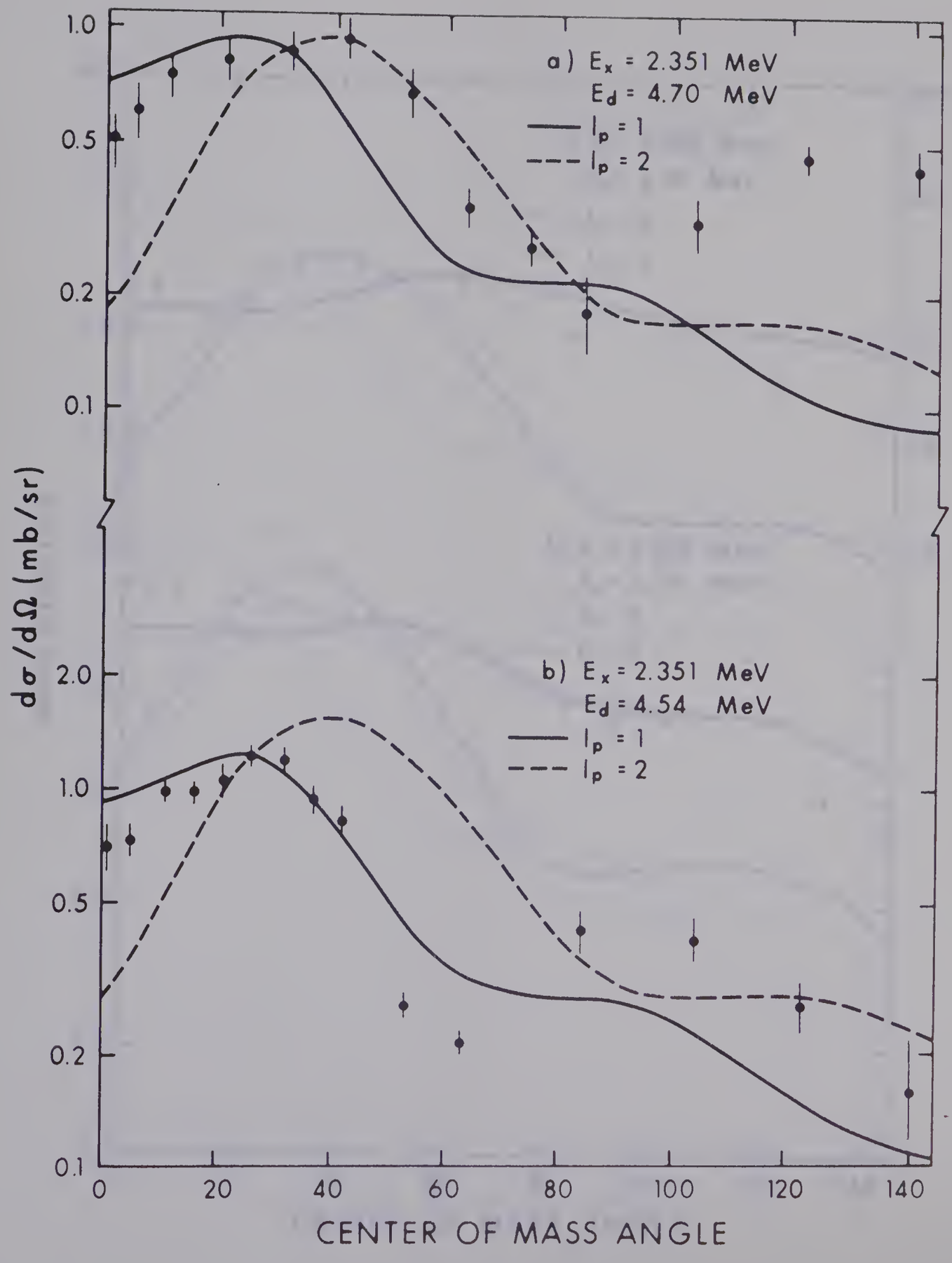
a) E_x = 2.351 MeV
E_d = 4.70 MeV
l_p = 1
l_p = 2
b) E_x = 2.351 MeV
E_d = 4.54 MeV
l_p = 1
l_p = 2
dσ/dΩ (mb/sr)
CENTER OF MASS ANGLE
1.0
0.5
0.2
0.1
2.0
1.0
0.5
0.2
0.1
0
20
40
60
80
100
120
140

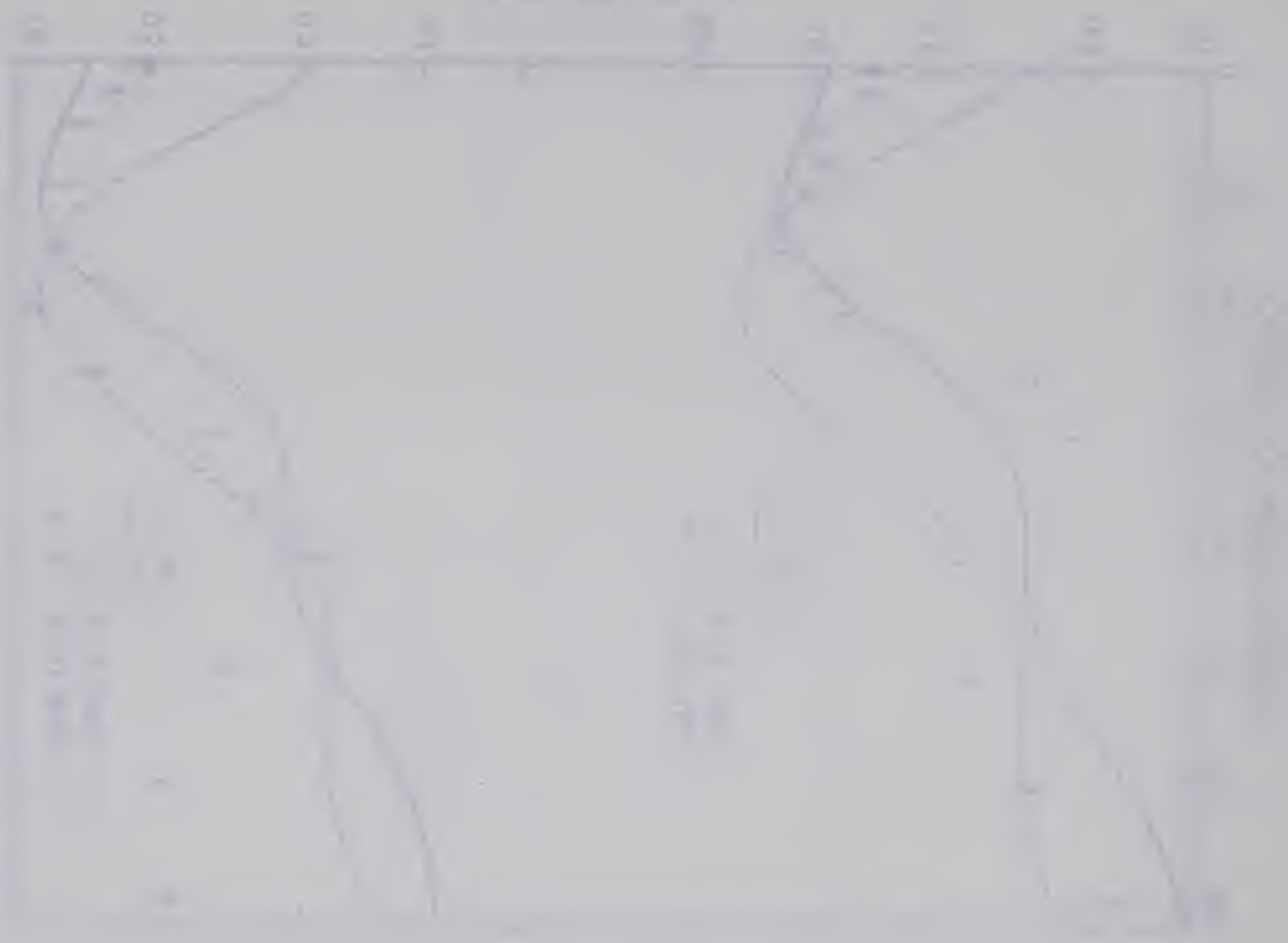

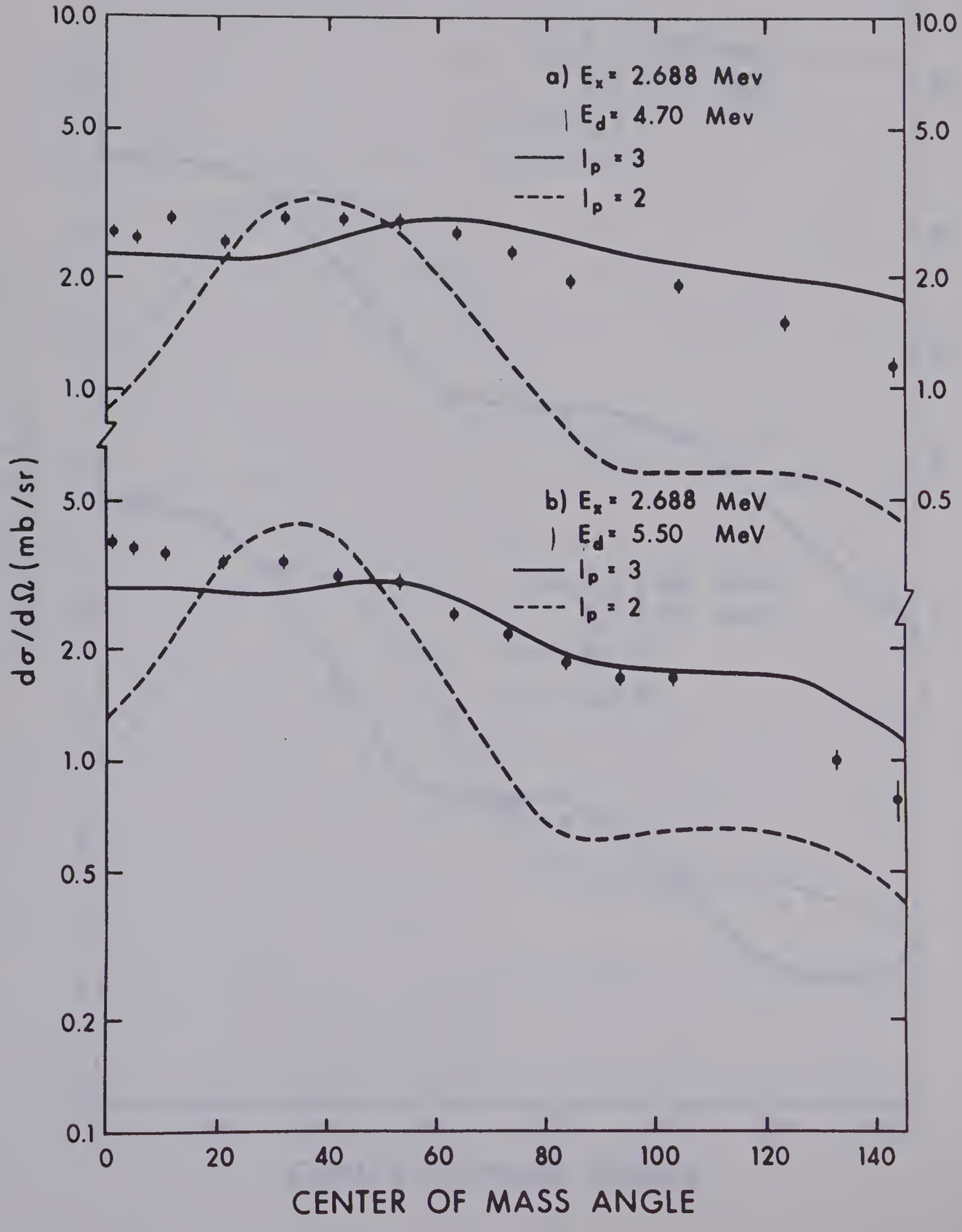
a) E_x = 2.688 Mev
E_d = 4.70 Mev
l_p = 3
l_p = 2
b) E_x = 2.688 MeV
E_d = 5.50 MeV
l_p = 3
l_p = 2
dσ/dΩ (mb/sr)
CENTER OF MASS ANGLE
10.0
5.0
2.0
1.0
0.5
0.2
0.1
0
20
40
60
80
100
120
140

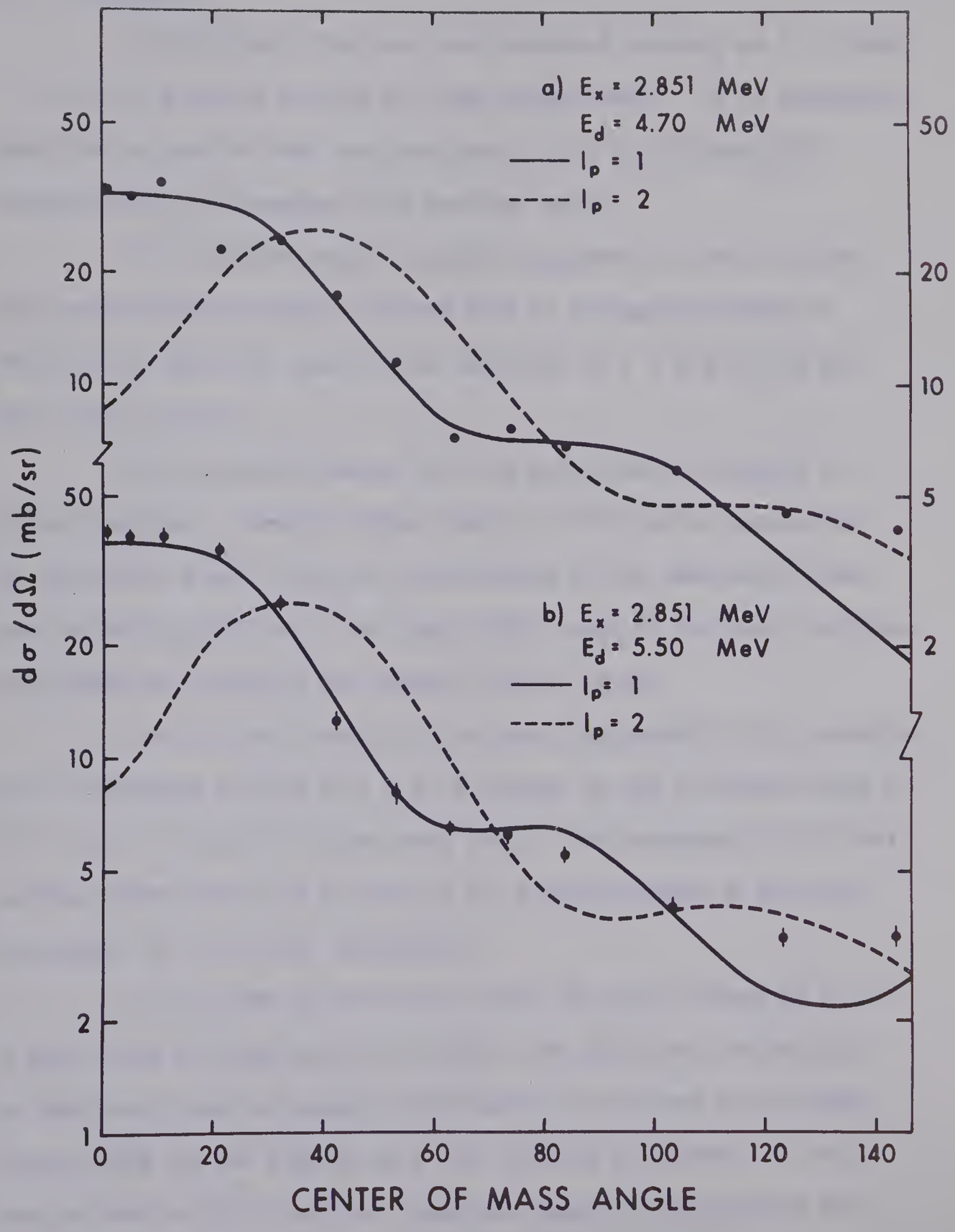
a) E_x = 2.851 MeV
E_d = 4.70 MeV
l_p = 1
l_p = 2
b) E_x = 2.851 MeV
E_d = 5.50 MeV
l_p = 1
l_p = 2
dσ/dΩ (mb/sr)
CENTER OF MASS ANGLE
50
20
10
5
2
1
0
20
40
60
80
100
120
140

4.3 Discussion

Satisfactory fits have been obtained assuming an $l = 2$ and $l = 0$ for the ground and the 0.81 MeV respectively. It is therefore possible to confirm that the spin-parity (J^{π}) is $3/2^{+}$ and $1/2^{+}$ respectively, in agreement with previous work.

The 1.99 MeV state is weakly populated in this reaction. The angular distributions obtained show no stripping pattern so that we are unable to resolve the ambiguity of J = 5/2 or 7/2 for this level (Pr 67).

All the levels above the 1.99 MeV state are unbound to proton emission. However higher levels of ^{33}Cl can be considered as "partially bound" owing to the presence of the combined Coulomb and centrefugal barrier. The code, DWUCK, used in this work includes the option of analyzing the unbound "bound" states.

The 2.35 MeV level is also weakly populated in this reaction and is expected to have an $l = 2$ in analogy to the 2.313 MeV state in ^{33}S. An $l = 1$ and $l = 2$ have been tried. The presence of ^{17}F first excited state which has a strong $l = 0$ transition made a definite assignment of this level impossible.

In the (^{3}He,d) work of A. Graue (Gr 66) l-values of 2 and 3 were tried for the level at 2.69 MeV. No definite l-value could be obtained since the angular distributions predicted by the DWBA theory used for the (^{3}He,d) work are not much different. In the present work we find that the predicted angular distributions for $l = 2$ and 3 are quite different for the (d,n) reaction. It is

TABLE 4-2

State	Present Work†			(^{3}He,d)††		Shell Model†††	
	Assumed J^π	S E_d=4.70 MeV	S E_d=5.50 MeV	Assumed J^π	S $E_{^3He}$=12 MeV	J^π	S
GND	$3/2^+$	0.87	0.66	$3/2^+$	0.47	$3/2^+$	0.820
0.81	$1/2^+$	0.15	0.13	$1/2^+$	0.22	$1/2^+$	0.240
1.99	$5/2^+$	0.02				$5/2^+$	0.0
2.35	$3/2^+$	0.08				$3/2^+$	0.013
2.69	$7/2^-$	0.42	0.33	$7/2^-$	0.75		
2.85	$3/2^-$	0.43	0.42	$3/2^-$	0.74		

† The values of S are believed to be reliable to within 25% taking into account both experimental errors in the cross section and the uncertainties in the analysis procedure.

†† (Gr 66) The uncertainties in S are ± 30%.

††† (Gl 64)

clear from fig. 4-5 that the 2.69 MeV level shows an angular distribution consistent with $\ell = 3$ and a level spin of $5/2^-$ or $7/2^-$. The 2.69 MeV state is very likely to be the $1f_{7/2}$ state expected in this range of excitation energy. The theoretical work of Watson and Lee (Wa 67) predicts a $1f_{7/2}$ state in ^{33}Cl at 2.75 MeV excitation.

The 2.85 MeV state is known from gamma ray work (Va 58, Pr 67) to be a doublet with spins $5/2^+$ and $3/2^-$. The angular distributions obtained in the present work shows that the $\ell = 1$ member is much stronger than that of the $\ell = 2$. This result agrees with that obtained by Graue.

The absolute spectroscopic factors extracted using the data at 4.70 and 5.50 MeV are given in table 4-2. The values of S obtained at the two energies agree within the indicated uncertainties.

The experimentally determined spectroscopic factors depend on the cross section predicted by the DWBA theory. It is important to find out how sensitive the calculated cross section, and hence the spectroscopic factors, are to changes in some of the optical model parameters, the incorporation of nonlocality approximation, and the omission of finite range correction. This has been investigated and the results are presented in table 4-3. S seems to be insensitive to spin-orbit effects, finite range correction and to large changes in the imaginary well depth for the deuteron. However, the addition of nonlocality creates a change of $\leq$ 27% in S but it should be noted that its incorporation is only an approximation. We can then see that although the deuteron optical parameters are obtained from data at bombarding energy much higher than that used in the present experiment, the resultant spectroscopic factors should not be greatly affected by this.

Change in Optical Model Parameters	Percentage change in $S(E_d=4.7$ MeV)			
	GND $\ell=2$	0.81 $\ell=0$	2.69 $\ell=3$	2.85 $\ell=1$
With W_D = 14.6 MeV (62% change)	+6	+16	+10	+9
With nonlocal potentials†	-25	-27	-20	-16
Without spin-orbit for the deuteron	+5	+6	+3	+4
Without spin-orbit for the Captured Proton	+20	0	+16	+3
Without spin-orbit for the neutron	-3	+2	+1	+1
With zero range	+3	+3	+2	+5

TABLE 4-3

Sensitivity of the Spectroscopic Factors to the Form and Parameters of the DWBA Calculation

† $\beta_n = \beta_p = 0.85$ fm. $\beta_d = 0.54$ fm.

For comparison, the values of S obtained by Graue (Gr 66) using the (^{3}He,d) reaction are also shown in table 4-2. Although these values are somewhat different from what we have measured the general trend of both sets is in agreement. Since the spin of the 2.69 MeV state is not known Graue reported the value of the strength function (2J+1)S rather than the spectroscopic factor. Thus to compare his result for this level with that of the present work we have calculated S assuming $J^{\pi} = 7/2^{-}$.

4.4 Shell Model Description for ^{33}Cl Nucleus

Glaudemans et al. (Gl 64) have carried out shell model calculations for levels of even parity in nuclei in the mass range 29 to 40. An inert ^{28}Si Core is assumed with a two-particle interaction of the outer nucleons in the $2s_{1/2}$ and $1d_{3/2}$ shells. Mixing of all possible configurations in these shells is taken into account. The level scheme predicted by these calculations for A=33 is shown in fig. 4-7. By using a delta function as the effective two-nucleon interaction acting only in the nuclear surface as has been suggested by Green and Moszkowski (Gr 65) , Glaudemans et al. (Gl 66) recalculated the excitation energies, and the new energy values agree very well with the experimental energies. However, the odd parity levels are not predicted by these calculations. Erne (Er 66) has performed shell model calculations of levels of odd parity in the region of the $1d_{3/2}$ shell nuclei. An inert ^{32}S Core is assumed with a residual two-particle interaction of the outer nucleons. Only one nucleon is considered to be in the $1f_{7/2}$ shell, while the others are in the $1d_{3/2}$

Figure 4-7. Comparison of the theoretical energy levels and spins with the experimental data on the low-lying states in the ^{33}Cl nucleus.

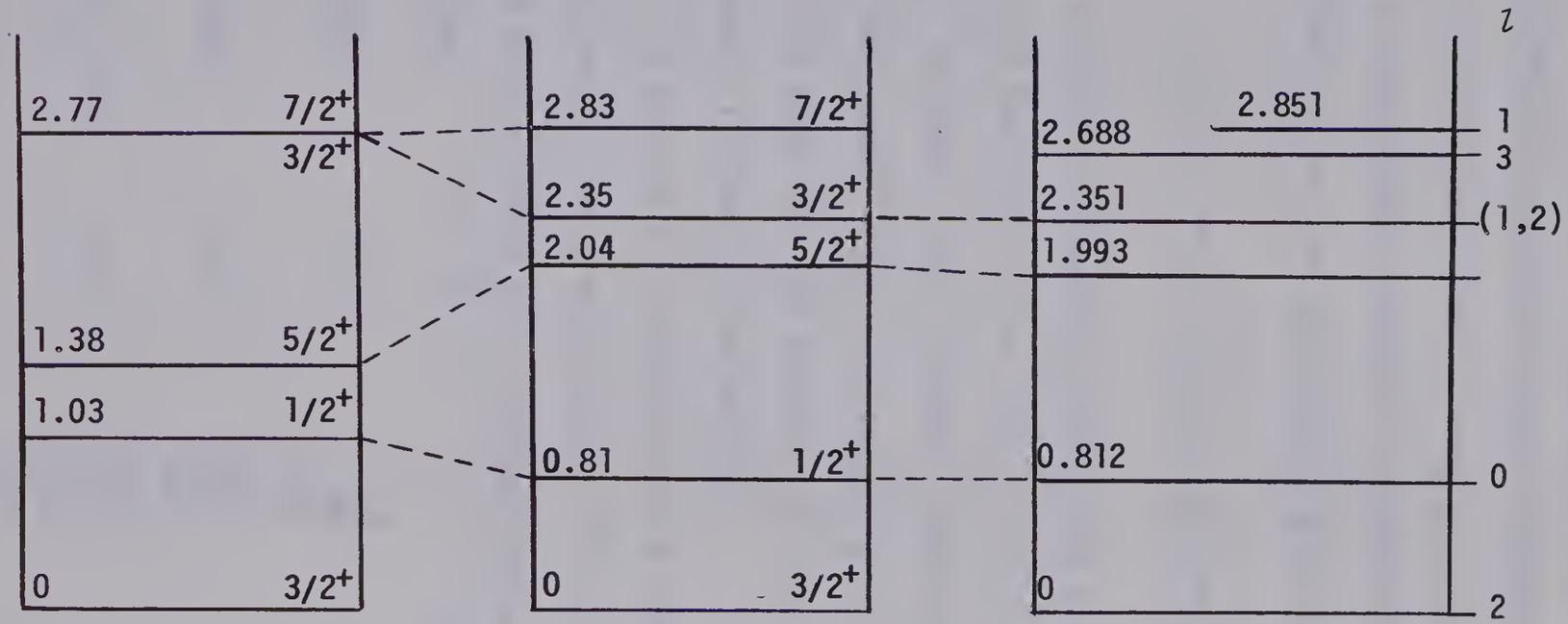
2.77
7/2+
3/2+
1.38
5/2+
1.03
1/2+
0
3/2+
2.83
7/2+
2.35
3/2+
2.04
5/2+
0.81
1/2+
0
3/2+
2.851
2.688
2.351
1.993
0.812
0
1
3
(1,2)
0
2
THEORY
(G1 64)
THEORY
(G1 66)
EXPERIMENT
Present Work

^{33}Cl

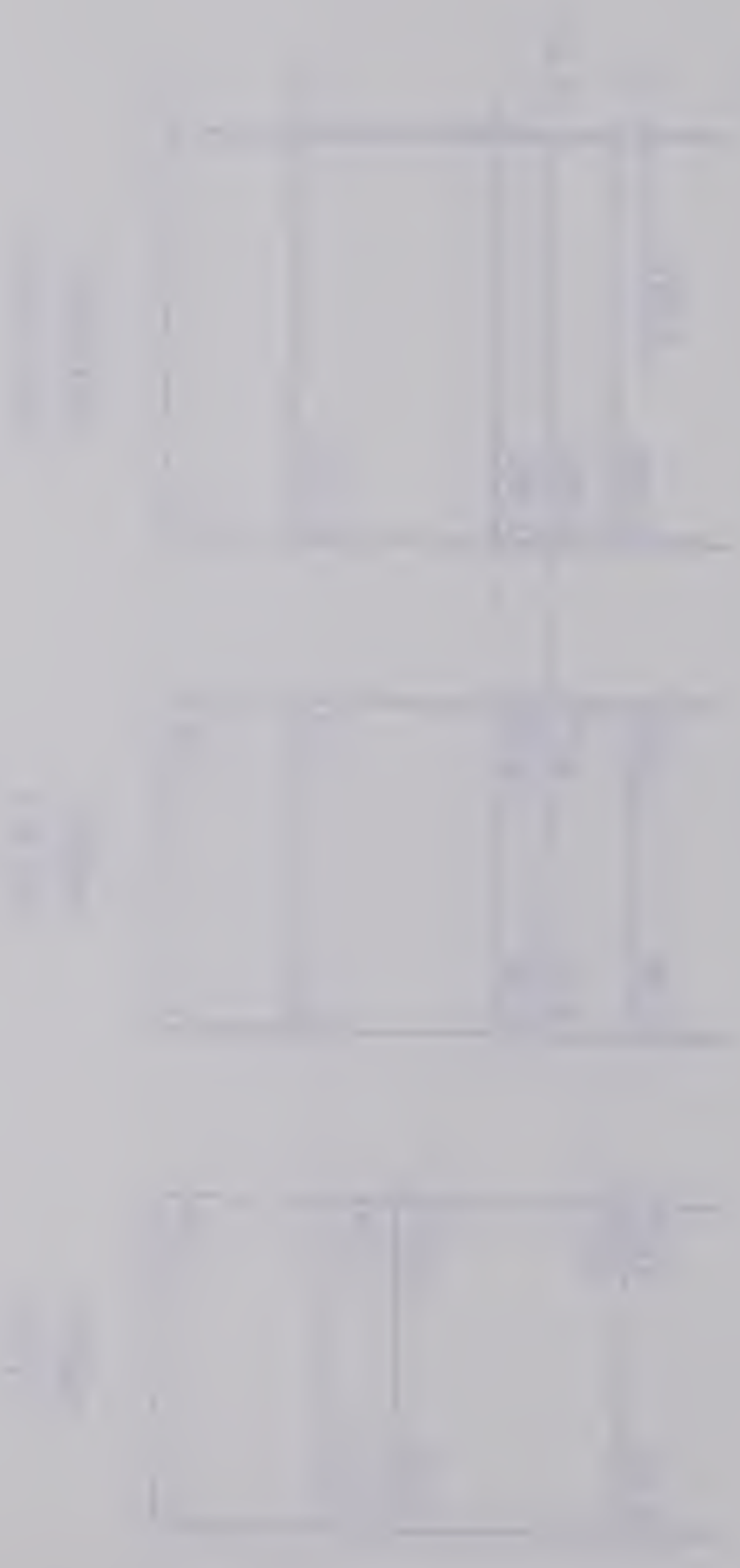

shell. According to these calculations, the $1f_{7/2}$ state in ^{33}Cl is predicted at 2.94±0.5 MeV excitation. The level observed in the present work at 2.69 MeV excitation is most probably the $1f_{7/2}$ state.

It is interesting to find out how the shell model can be used to make a quantitative analysis of spectroscopic factors. S is defined theoretically as an overlap integral given by:

$$S^{\frac{1}{2}}(lj) = (A+1)^{\frac{1}{2}} \int \Phi(J_i j l)\ \psi_{J_f}\ d(A+1)$$

where Φ is the wave function constructed by the vector coupling to spin J_f of a particle in the state lj to the target wave function of spin J_i. The symbol d(A+1) denotes integration over the (A+1) nucleons in the final state. Thus by overlapping the wave functions predicted by the shell model for the initial and final states, predictions of spectroscopic factors can be obtained.

In the early calculations of Glaudemans et al. (Gl 64), the wave functions of the ground state of ^{32}S and the predicted states of ^{33}Cl have the following major configurations: -

Level	J^π	Configuration		
^{32}S(GND)	0^+	s4 00 -496	s2d2 0101 +391	
^{33}Cl(GND)	$3/2^+$	s4d1 00$\bar{3}\bar{1}$ -621	s2d3 01$\bar{3}\bar{1}$ -160	s2d3 01$\bar{3}\bar{3}$ -127
^{33}Cl(1.03)	$1/2^+$	s3d2 11$\bar{1}$0 -112	s3d2 11$\bar{0}$1 +732	s1d4 11$\bar{0}$0 -125
^{33}Cl(1.38)	$5/2^+$	s3d2 11$\bar{2}$1 -665	s1d4 11$\bar{2}$1 -118	
^{33}Cl(2.77)	$3/2^+$	s3d2 11$\bar{1}$0 +183	s2d3 01$\bar{3}\bar{1}$ -354	s2d3 10$\bar{3}\bar{1}$ +242

where the notation of Glaudemans et al. has been used. The number in brackets under the first column refer to the calculated excitation energy of the level.

Since the wave functions have been determined, the spectroscopic factors for the stripping reaction $^{32}S(d,n)^{33}Cl$ could be calculated. The general expressions for S have been discussed by Macfarlane and French (Ma 60a). The values of S calculated by Glaudemans et al. (Gl 64) are presented in table 4-2.

The value of S for the ground state agrees with our result. The predicted value of S for the first excited state is a factor of 2 higher than the measured value. With the assumption that only $2s_{1/2}$ and $1d_{3/2}$ nucleons take part in the stripping process, the transition to the second excited state is impossible due to angular momentum relation. A small value of S has been predicted for the third excited state. The calculated spectroscopic factors for the second and third excited states are consistent with the observed weak transition to the 1.993 and 2.351 MeV states.

CHAPTER V

CONCLUSION

Three levels in ^{33}Cl at 1.993, 2.351 and 2.688 MeV excitation has been seen for the first time in the $^{32}S(d,n)^{33}Cl$ reaction. These results confirm those obtained recently using (^{3}He,d) and (p,γ) reactions on ^{32}S. We do not observe states at 2.1 and 2.5 MeV as reported in previous (d,n) work.

Angular distribution study confirms the previous spin-parity assignment of $3/2^{+}$ and $1/2^{+}$ for the ground and 0.812 MeV states, respectively. Also, it confirms that one member of the known doublet at 2.85 MeV observed in (p,γ) experiments has a spin-parity of $3/2^{-}$.

For the weakly populated level at 1.993 MeV no ℓ-value could be obtained due to the absence of stripping structure in its angular distribution. An ambiguity also remains of ℓ=1 or 2 for the level at 2.351 MeV excitation.

An ℓ=3 has been obtained for the level at 2.688 MeV and hence its spin is limited to be $5/2^{-}$ or $7/2^{-}$.

The spectroscopic factor predicted for the ground state using shell model calculations agrees with what we have measured. A qualitative agreement has been obtained for the 0.812, 1.993 and 2.351 MeV states. This suggests that ^{33}Cl nucleus can be well described by a ^{28}Si core with outer nucleons in the $2s_{1/2}$ and $1d_{3/2}$ shells.

REFERENCES

Bu 67 M.B. Burbank; M.Sc. Thesis, University of Alberta (unpublished) (1967).

Da 66 W. Davies; Ph.D. Thesis, University of Alberta (unpublished) (1966).

Da 68 N.E. Davison; Hauser-Feshbach Calculations, Nuclear Research Center, internal report, Physics Department, University of Alberta (1968).

Da 68a N.E. Davison; Ph.D. Thesis, University of Alberta (unpublished) (1969).

Da 69 N.E. Davison and R. Humphries; Plot and Print Program, Nuclear Research Center, internal report, Physics Department, University of Alberta (1969).

En 67 P.M. Endt and C. van der Leun, Nucl. Phys. A105 (1967) 1.

Er 66 F.C. Erné, Nucl. Phys. 84 (1966) 91.

Ge 67 D.A. Gedcke and W.J. McDonald, Nucl. Inst. and Meth. 55 (1967) 377.

Ge 67a D.A. Gedcke and W.J. McDonald, Nucl. Inst. and Meth. 56 (1967) 148.

Gl 64 P.W.M. Glaudemans, G. Wiechers and P.J. Brussaard, Nucl. Phys. 56 (1964) 548.

Gl 66 P.W.M. Glaudemans, B.H. Widenthal and J.B. McGrory, Phys. Lett. 21 (1966) 427.

Gr 65 I.M. Green and S.A. Moszkowski, Phys. Rev. 160 (1967) 925.

Gr 66 A. Graue, Physica Norvegica 2 (1966) 7.

Gr 67 T.B. Grandy; Ph.D. Thesis, University of Alberta (unpublished) (1967).

Gr 68 T.B. Grandy, W.J. McDonald, W.K. Dawson and G.C. Neilson, Nucl. Phys. A111 (1968) 469.

Ha 52 W. Hauser and H. Feshbach, Phys. Rev. 87 (1952) 366.

Ho 66 C.E. Hollandsworth, F.O. Purser, Jr., J.R. Sawers, Jr. and R.L. Walter, Phys. Rev. 150 (1966) 825.

Ku 67 P.D. Kunz, University of Colorado, private communication.

Ma 60 B.E.F. Macefield and J.H. Towle, Proc. Phys. Soc. 76 (1960) 56.

Ma 60a M.H. Macfarlane and J.B. French, Revs. Mod. Phys. 32 (1960) 567.

Mc 67 W.J. McDonald and D.A. Gedcke, Nucl. Inst. and Meth. 55 (1967) 1.

Mi 53 R. Middleton, F.A. El-Bedewi and C.T. Tai, Proc. Phys. Soc. A66 (1953) 95.

Mo 67 C.E. Moss, Bull. Am. Phys. Soc. 12 (1967) 914.

Mu 67 S. Mubarakmand and B.E.F. Macefield, Nucl. Phys. A98 (1967) 82.

Ob 66 A.W. Obst; M.Sc. Thesis, University of Alberta (unpublished) (1966).

Pe 66 C.M. Perey, F.G. Perey, Phys. Rev. 152 (1966) 923.

Pr 67 F.W. Prosser, Jr. and J.W. Gordon, Bull. Am. Phys. Soc. 12 (1967) 572 and AEC Report COO-1120-71, University of Kansas (unpublished).

Ro 66 L. Rosen; 'Second International Symposium on Polarization Phenomena of Nucleons' (1966) 278.

Sa 64 G.R. Satchler, Nucl. Phys. 55 (1964) 1.

Sm 65 W.R. Smith; Oak Ridge National Laboratory Internal Report ORNL-TM-1234.

Sm 68 D.L. Smith, R.G. Polk and T.G. Miller, Nucl. Inst. and Meth. 64 (1968) 157.

St 56 L. Stewart, G.M. Frye, Jr. and L. Rosen, Bull. Am. Phys. Soc. 1 (1956) 93.

Te 66 J.W. Tepel, Nucl. Inst. and Meth. 40 (1966) 100.

To 61 W. Tobocman, Theory of Direct Nuclear Reaction (Oxford University Press, New York, 1961).

Va 58 C. van der Leun and P.M. Endt, Physica 24 (1958) 1095.

Wa 66 D.D. Watson, Rev. Sci. Inst. 37 (1966) 1605.

Wa 67 D.D. Watson and F.D. Lee, Phys. Lett. 25B (1967) 472